Available online at www.sciencedirect.com
SCIENCE DIRECT®
Planetary and Space Science 53 (2005) 1243–1262
Planetary and Space Science
www.elsevier.com/locate/pss

The origin of the CN radical in comets: A review from observations and models

N. Fray[a,*], Y. Bénilan[a], H. Cottin[a], M.-C. Gazeau[a], J. Crovisier[b]

[a]*Laboratoire Interuniversitaire des Systèmes Atmosphériques (LISA), UMR 7583 du CNRS, Universités Paris 7 and Paris 12, C.M.C., 61 Avenue du Général de Gaulle, 94010 Créteil Cedex, France*
[b]*Observatoire de Paris-Meudon, 92195 Meudon, France*

Received 18 September 2003; received in revised form 30 May 2005; accepted 24 June 2005
Available online 15 August 2005

Abstract

The origin of CN radicals in comets is not completely understood so far. We present a study of CN and HCN production rates and CN Haser scale lengths showing that: (1) at heliocentric distances larger than 3 AU, CN radicals could be entirely produced by HCN photolysis; (2) closer to the Sun, for a fraction of comets CN production rates are higher than HCN ones whereas (3) in the others, CN distribution cannot be explained by the HCN photolysis although CN and HCN production rates seem to be similar. Thus, when the comets are closer than 3 AU to the Sun, an additional process to the HCN photolysis seems to be required to explain the CN density in some comets.

The photolysis of HC_3N or C_2N_2 could explain the CN origin. But the HC_3N production rate is probably too low to reproduce CN density profile, even if uncertainties on its photolysis leave the place for all possible conclusions. The presence of C_2N_2 in comets is a reliable hypothesis to explain the CN origin; thus, its detection is a challenging issue. Since C_2N_2 is very difficult to detect from ground-based observations, only in situ measurements or space observations could determine the contribution of this compound in the CN origin.

Another hypothesis is a direct production of CN radicals by the photo- or thermal degradation of complex refractory organic compounds present on cometary grains. This process could explain the spatial profile of CN inside jets and the discrepancy noted in the isotopic ratio $^{14}N/^{15}N$ between CN and HCN. Laboratory studies of the thermal and UV-induced degradation of solid nitrogenated compounds are required to model and validate this hypothesis.

Keywords: Astrochemistry; Comets; Molecules

1. Introduction

The CN radical was one of the first species, with the C_2 radical, to be detected in the cometary environment at the end of the XIXth century. The detection of HCN was first claimed by Huebner et al. (1974) in comet C/1973 E1 (Kohoutek). Whereas this detection is controversial, because of the low signal-to-noise ratio of the signal, it seemed to explain the origin of the CN radical since Combi and Delsemme (1980b) had shown that the Haser scale length of CN production was coherent with HCN photolysis. Subsequently, HCN has been securely detected in comet 1P/Halley by three independent teams (Despois et al., 1986; Schloerb et al., 1986; Winnberg et al., 1987).

Using a better value of the expansion velocity of the gas in the coma, Bockelée-Morvan et al. (1984) showed that the HCN production rates upper limits were smaller than the CN ones and that the CN parent Haser scale length could not be associated with the HCN photo-dissociation alone (Bockelée-Morvan and Crovisier, 1985). After this publication, the origin of the cometary

*Corresponding author. Tel.: +33 0 1 45 17 15 37; fax: +33 0 1 45 17 15 64.
E-mail address: fray@lisa.univ-paris12.fr (N. Fray).

0032-0633/$ - see front matter © 2005 Elsevier Ltd. All rights reserved.
doi:10.1016/j.pss.2005.06.005

CN radicals became highly debated and several gaseous molecules have been proposed as a second parent: C_2N_2 (Bockelée-Morvan and Crovisier, 1985; Festou et al., 1998), HC_3N (Bockelée-Morvan and Crovisier, 1985; Krasnopolsky, 1991) or even C_4N_2 (Krasnopolsky, 1991). Another hypothesis is that CN could be directly emitted from grains. This was first proposed in order to explain CN jets in comet 1P/Halley (A'Hearn et al., 1986a). Furthermore, comparative studies between comets supported the dust as CN source (Newburn and Spinrad, 1989; A'Hearn et al., 1995), since the CN and dust production rates seem to be correlated. Other authors, like Klavetter and A'Hearn (1994), proposed that CN could be produced by another extended source: a source other than the nucleus or a gaseous parent.

In this paper, we present a review about available data of CN radical observations and current interpretations in order to extract a global view of the recurrent problem: the origin of the cometary CN radical.

We first present a compilation of the published CN Haser scale lengths from which we derive an average value of CN parent scale length at 1 AU at minimum solar activity. This average value is compared to the photolysis data of several possible gaseous parent molecules. Then we compare the HCN and CN production rates in several comets and discuss the implications of the production rate uncertainties. Finally, we study the case of the CN jets.

2. CN scale lengths

In order to constrain the formation process(es) of CN radicals in comets, one can study its distribution in the coma. In a first approximation, one can consider that this distribution is directly related to the kinetics of the formation process(es). Thus, it can be compared with the destruction process of HCN and other CN-bearing molecules.

According to the Haser (1957) model, such a distribution can be modeled with two scale lengths: a "parent scale length" (l_p) and a "daughter scale length" (l_d). The hypotheses of this model are that: (1) the production rate is in steady state; (2) CN radicals are produced by the photodissociation of a single parent molecule and (3) the motion from the nucleus is radial for both parent and daughter molecules. Then, the density per unit volume follows the law

$$n(r) = \frac{Q_p}{4\pi r^2 V_{gas}} \frac{l_d}{l_p - l_d} (e^{-r/l_p} - e^{-r/l_d}), \quad (1)$$

where $n(r)$ is the density of CN radicals at a distance r from the nucleus, Q_p the production rate of the parent molecule and V_{gas} the expansion velocity of the daughter molecules in the coma. In this model, the parent scale length is the characteristic length of CN production and the daughter scale length is the characteristic length of CN dissociation. In a first approximation, one can consider that the parent scale length is related to the photodissociation rate of the parent molecule β_p through $l_p = V_{gas}/\beta_p$; but as we will see in Section 4, a better estimation is achieved with the model of Combi and Delsemme (1980a), which takes into account the excess energy acquired by the fragment during the photodissociation process.

As the photodissociation rates vary as R_H^2 (where R_H is the heliocentric distance in astronomical unit) and the expansion velocity as approximately as $R_H^{-0.5}$ (Cochran and Schleicher, 1993; Biver et al., 1999a), if we consider a pure Haser model, then the scale lengths should vary approximately as $R_H^{1.5}$. If we use the model of Combi and Delsemme (1980a), we find that the parent scale length should vary approximately as $R_H^{1.4}$ (see Section 4).

We have compiled all the CN Haser parent and daughter scale lengths that we have found in the literature. This allows us to constrain a mean value at 1 AU as well as the variation of these scale lengths as a function of the heliocentric distance of the parent and daughter scale lengths. The comparison with the observed distribution and photodissociation rates of the possible gaseous parent molecules is then discussed using the model of Combi and Delsemme (1980a).

2.1. Compilation of the CN scale lengths

We have compiled 104 values of CN Haser parent scale lengths (Combi, 1978; Combi and Delsemme, 1980b; Delsemme and Combi, 1983; Fink et al., 1991; Meredith et al., 1992; Newburn and Spinrad, 1984; Rauer et al., 2003; Umbach et al., 1998; Woodney et al., 2002). For each value, we have quoted the heliocentric distance (R_H) and the date of the observation. Fig. 1a shows the CN parent scale lengths as a function of the heliocentric distance. As one can see in this figure, there is a great dispersion between these values, which are indeed bracketed by the functions $6 \times 10^3 R_H^2$ and $5.2 \times 10^4 R_H^2$ km.

We have also compiled 38 values of the CN daughter scale lengths (Combi, 1978; Combi and Delsemme, 1980b; Fink et al., 1991; Meredith et al., 1992; Umbach et al., 1998; Woodney et al., 2002). As one can see in Fig. 2a, the CN daughter scale lengths as a function of the heliocentric distance also exhibit a great dispersion: they lie between $4 \times 10^4 R_H^{1.4}$ and 8.5×10^5 km$R_H^{1.4}$.

2.2. Reduction of the scale lengths to the minimum of solar flux

One possible source of the dispersion in the values of CN scale lengths could be the change of solar activity between the different periods of observations. Meredith et al. (1992) have shown that the measured values at

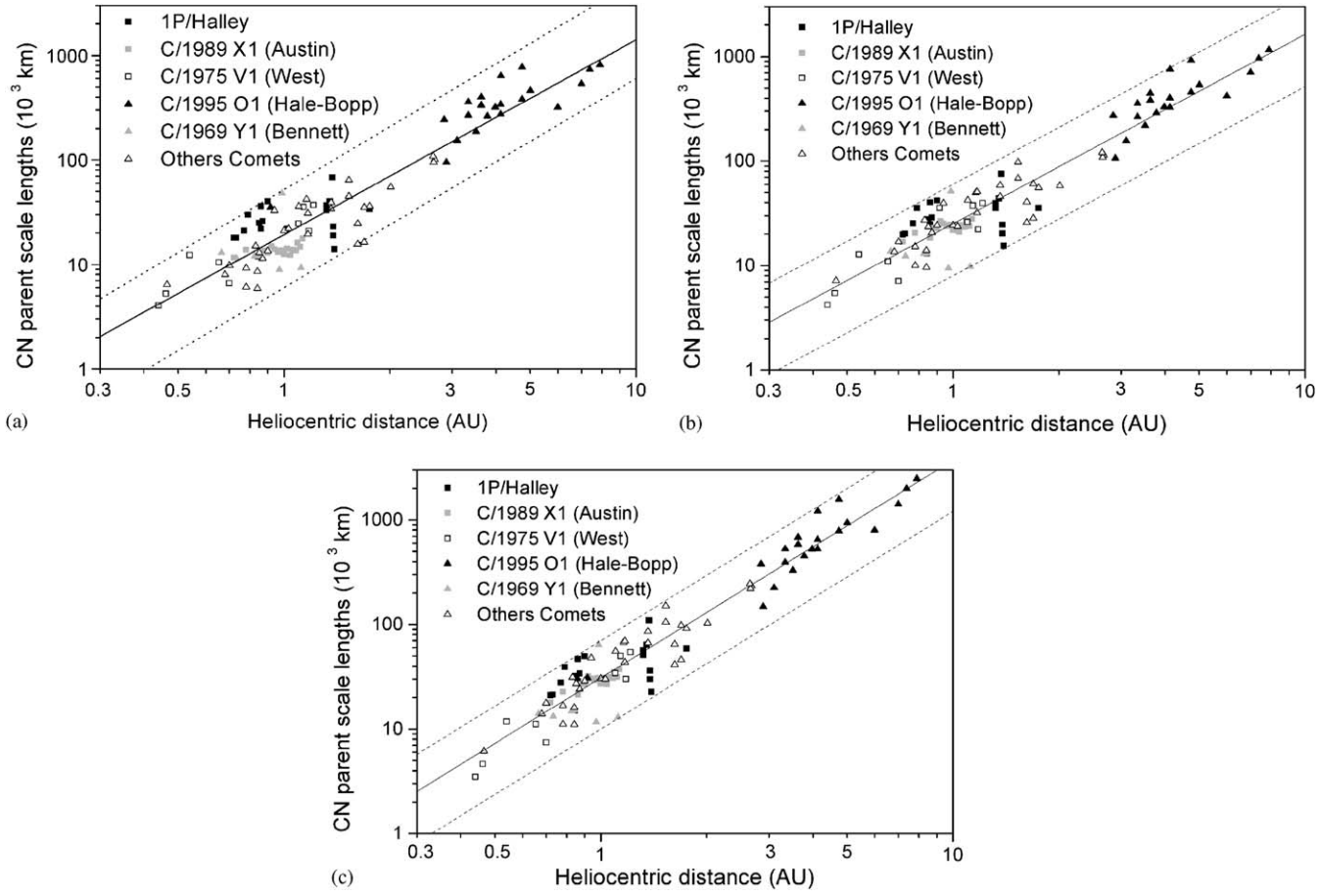

Fig. 1. (a) Original CN parent scale lengths as a function of the heliocentric distance R_H. The black line is the best fit ($1.93 \times 10^4 R_H^{1.86}$ km) and the dotted lines represent the functions $6 \times 10^3 R_H^2$ and $5.2 \times 10^4 R_H^2$ km. (b) CN parent scale lengths normalized to the minimum of solar flux as a function of the heliocentric distance R_H. The black line is the best fit ($2.5 \times 10^4 R_H^{1.8}$ km) and the dotted lines represent the functions $8 \times 10^3 R_H^{1.8}$ and $6 \times 10^4 R_H^{1.8}$ km. (c) CN parent scale lengths normalized to the minimum of solar flux and to an expansion velocity of 1 km s^{-1} (see text) as a function of the heliocentric distance R_H. The black line is the best fit ($3.1 \times 10^4 R_H^{2.1}$ km) and the dotted lines represent the functions $10^4 R_H^{2.1}$ and $7 \times 10^4 R_H^{2.1}$ km.

1 AU of parent scale lengths rise when the solar flux decreases.

So, in order to compare them with the photodissociation rates of parent molecules which are calculated for quiet Sun conditions, the CN parent scale lengths have been normalized to the minimum of solar activity.

We used the formula

$$l_{norm} = l_{orig}(F/F_{min}),$$

where l_{orig} is the original scale lengths, l_{norm} the "normalized" scale lengths, i.e., those which have been recalculated and F the flux at Lyman α at the date of the observation. We have used the Lyman α flux calculated by Woods et al. (2000), available on the site of the NOAA (ftp://ftp.ngdc.noaa.gov/STP/SOLAR_DATA/SOLAR_UV/SOLAR2000/Five_cycle_v1_23a.txt). As one can see in Fig. 1b, the dispersion of the parent scale lengths is not reduced by this operation, and at this stage, a similar result is found for the daughter scale lengths. However, the mean value of the normalized scale length are larger, because the solar flux F is larger than F_{min} (see Section 2.5).

2.3. Reduction of the scale lengths to an expansion velocity of 1 km s^{-1}

Another possible source of dispersion in the value of CN scale lengths could be the difference of the gas expansion velocity between more or less active comets (see Bockelée-Morvan et al., 1990; Combi, 2002). For example, the expansion velocity observed in the very active C/1995 O1 (Hale-Bopp) was greater than in any others comets observed up to now. So, we have reduced all the scale lengths to a gas expansion velocity of 1 km s^{-1}, considering that the expansion velocity in all comets was the one measured in 1P/Halley ($0.85 R_H^{-0.5}$ km s^{-1}; Cochran and Schleicher, 1993) except

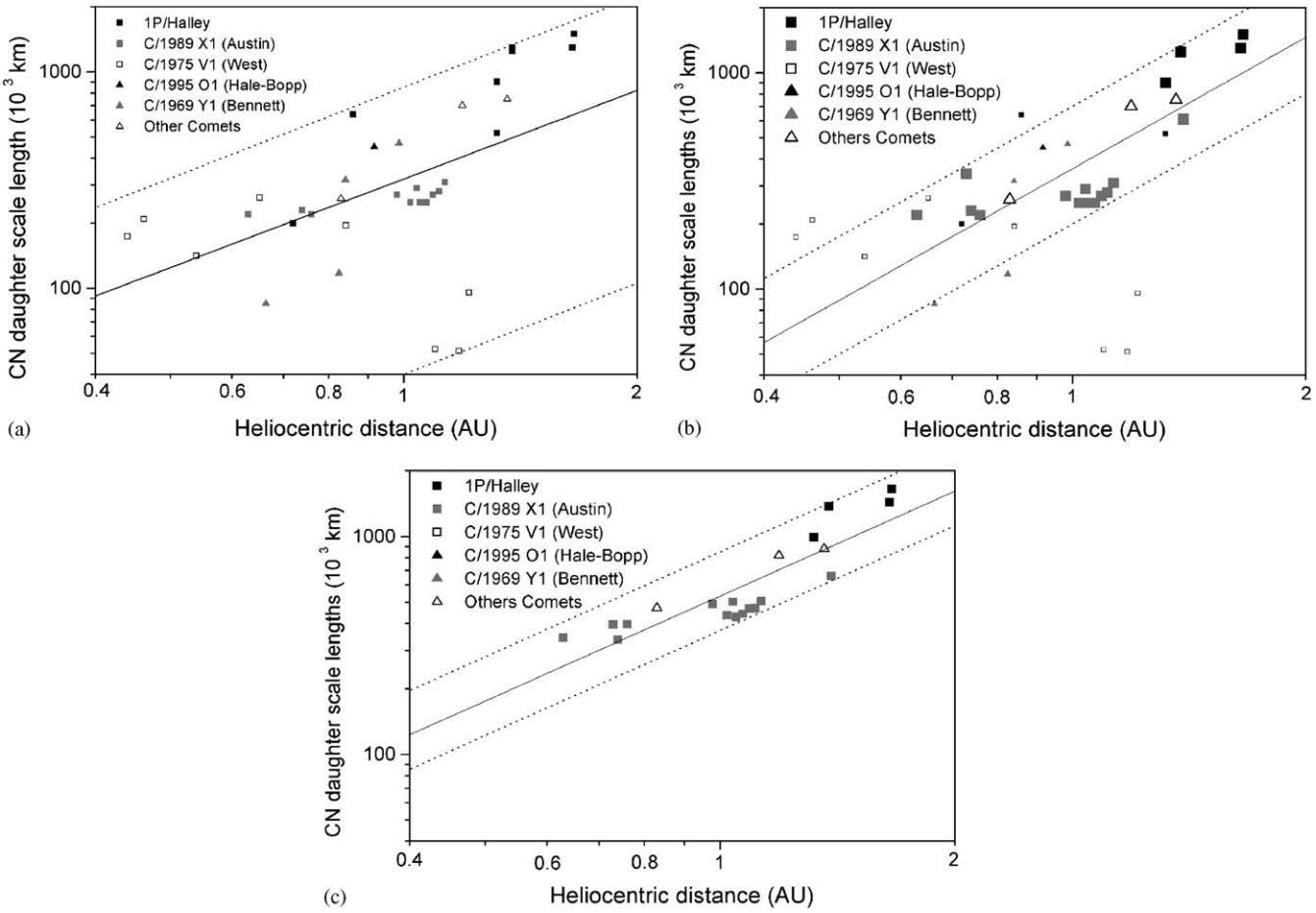

Fig. 2. (a) Original CN daughter scale lengths as a function of the heliocentric distance R_H. The black line is the best fit ($3.2\times10^5 R_H^{1.4}$ km) and the dotted lines represent the functions $4\times10^4 R_H^{1.4}$ and $8.5\times10^5 R_H^{1.4}$ km. (b) CN daughter scale lengths as a function of the heliocentric distance R_H. The bigger symbols represent the values that were obtained from a wide field of view, whereas the smaller symbols are daughter scale lengths obtained from profiles for which the extension of the measurements was smaller than the derived daughter scale lengths. This selection allows us to reduce the dispersion observed on the measured CN Haser daughter scale lengths. The black line is the best fit on the selected values ($3.6\times10^5 R_H^2$ km) and the dotted lines represent the functions $2\times10^5 R_H^2$ and $7\times10^5 R_H^2$ km. (c) Similar to (b), but the CN daughter scale lengths have been normalized to the minimum of solar flux. The black line is the best fit ($5.33\times10^5 R_H^{1.6}$ km) and the dotted lines represent the functions $3.7\times10^5 R_H^{1.6}$ and $8.5\times10^5 R_H^{1.6}$ km.

in C/1995 O1 (Hale-Bopp), where it was $1.12 R_H^{-0.42}$ km s^{-1} (Biver et al., 2002).

We have presented the parent scale lengths normalized to the minimum of solar flux and an expansion velocity of 1 km s^{-1} in Fig. 1c. The dispersion of the values is still not reduced by the operation.

2.4. Possible origin of the dispersion of the values of the CN Haser scale lengths

We have shown that the changes in the solar flux or in the expansion velocity between more or less productive comets are not responsible for the dispersion observed on the measured parent CN scale lengths. Thus, another explanation of such dispersion of the CN Haser scale lengths could be that an artifact is introduced by the Haser model. Indeed, most spatial measurements only yield to a family of solutions consisting of numerous parent and daughter scale length pairs that yield equally good fits with the Haser model.

In order to illustrate this fact, we studied two CN spatial profiles. The first one was published by Womack et al. (1994) and was acquired on comet 1P/Halley on December 14, 1985 at 1.28 AU from the Sun. The measurements extend from 8×10^3 to 5×10^5 km from the nucleus (Fig. 3a). The second one was published by Fink et al. (1991) and was measured on comet 1P/Halley on January 11, 1986 at 0.86 AU. It extends from 4×10^3 to 9×10^4 km from the nucleus (Fig. 4a). For both profiles, we have searched the best fit with a Haser model by χ^2 minimizing. Figs. 3b and 4b represent the χ^2 which is achieved for each pairs of parent and daughter scale lengths for both profiles.

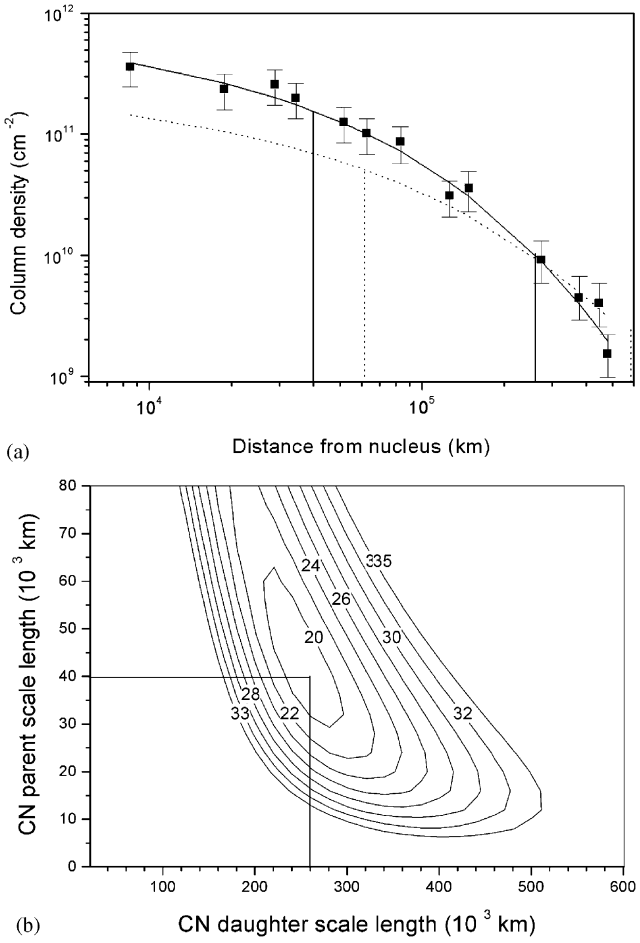

Fig. 3. (a) CN column density profile as a function of the projected distance from the nucleus observed by Womack et al. (1994) in comet Halley on December 14, 1985 at 1.28 UA from the Sun. The black line is the best fit with a Haser profile (the parent scale length is 40,000 km, the daughter scale length is 261,000 km; both these scale lengths have been represented as straight vertical lines). The χ^2 of this fit is 18.8 (see (b)). The dotted line is the best fit if we consider that HCN is the unique parent molecule of CN (the effective parent scale length is 6.22×10^4 km (see Fig. 11), the daughter scale length is 7.87×10^5 km (see (c) and Table 2); both these scale lengths have been represented as dotted vertical lines). The χ^2 of this second fit is 52.8. (b) The curves that are displayed correspond to the same value of the χ^2 which is achieved when we fit the profile presented in (a) with a Haser model as a function of the parent and daughter scale lengths. Best scale lengths to fit the profile presented in (a) with a Haser model are $l_p = 4 \times 10^4$ km and $l_d = 2.6 \times 10^5$ km (both these scale lengths are displayed as straight lines).

On the first set of measurements ($R_H = 1.28$ AU), the best fit is obtained for $l_p = 4 \times 10^4$ km and $l_d = 2.6 \times 10^5$ km, whereas for the second one ($R_H = 0.86$ AU), the best fit is achieved for $l_p = 3.8 \times 10^4$ km and $l_d = 2.1 \times 10^5$ km. Figs. 3a and 4a display both fits, respectively.

On the one hand, only couples of a small family (l_p, l_d) are solutions (Fig. 3b). Hence, the Haser scale lengths that are determined from this first profile, for which the extension of measurements (5×10^5 km) is greater than the derived daughter scale length (2.6×10^5 km), seem to be reliable. On the other hand, the second set of measurements can be fitted with a large number of parent and daughter scale lengths (Fig. 4b). Moreover, it allows us to point out the fact that the determination of the daughter Haser scale length with this second profile is not achievable with a good accuracy. Indeed, the extension of this second profile (up to 9×10^4 km from the nucleus) is smaller than the daughter scale length (about 3.2×10^5 km); hence, it could not be used to determine the daughter scale lengths.

These results show that only spatial profiles obtained with a telescope with a field of view extending further than the daughter scale length l_d allow one to determine parent and daughter scale lengths at the same time. That is the reason why, generally, when the extension of a spatial profile is shorter than the daughter scale length, a value of the daughter scale length is assumed in order to compute a parent scale length. So, if a wrong daughter value is assumed, then the resulting parent value is also likely incorrect.

2.5. Fit of the CN daughter scale lengths as a function of the heliocentric distance

Selecting only profiles taken with a wide enough field of view, we have kept 20 scale length values and rejected 18. This selection is presented in Fig. 2b (original scale lengths) and in Fig. 2c (scale lengths normalized to the minimum of solar flux).

This selection allows us to reduce the dispersion observed for the measurements on daughter scale lengths. The remaining dispersion could be due to short-term variation of the CN production rates. Indeed, some profiles that have an extension greater than 10^5 km from the nucleus exhibit some wavy structures characteristic of a time-dependent production rate related to the rotation of the nucleus (Combi and Fink, 1993; Combi et al., 1994). As the Haser model considers that the production rate is in steady state, these wavy structures could prevent a good determination of the scale lengths even if the extension of the profile is large.

Then, we have fitted the logarithm of the daughter scale length as a function of the logarithm of the heliocentric distance by a straight line. Three fits are presented in Fig. 2a, b and 2c, respectively, and the results are summarized in Table 2. For the original scale lengths, the best fit on the selected values is obtained for $l_d = 3.6 \times 10^5 R_H^2$ km (Fig. 2b). This mean value scaled at 1 AU and the heliocentric dependence are in accordance with the values previously published, which range from 2.1 to 4.2×10^5 km with an exponent of 2. On the other hand, the best fit obtained for the selected scale length normalized to the minimum of solar flux is

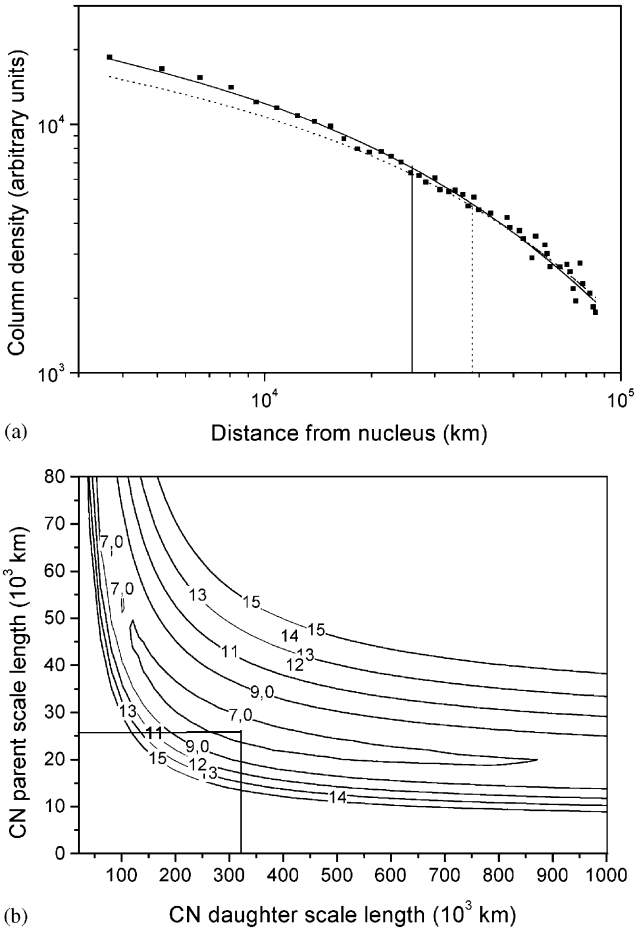

Fig. 4. (a) CN column density profile as a function of the projected distance from the nucleus observed by Fink et al. (1991) in comet Halley on January 11, 1986 at 0.86 UA from the Sun. The black line is the best fit with a Haser profile (the parent scale length is 2.6×10^4 km and displayed as a vertical straight line, the daughter scale length is 3.21×10^5 km and the χ^2 of this fit is 6.7). The dotted line is the best fit if we consider that HCN is the unique parent molecule of CN (the parent scale length is 3.8×10^4 km (see Fig. 11) and is displayed as a vertical dotted line, the daughter scale length is 2.65×10^5 km (see Fig. 2b and Table 2) and the χ^2 of this fit is 7.5). (b) The curves that are displayed correspond to the same value of the χ^2 which is achieved when we fit the profile presented in (a) with a Haser model as a function of the parent and daughter scale lengths. Best scale lengths to fit the profile presented in Fig. 3a with a Haser model are $l_p = 2.6 \times 10^4$ km and $l_d = 3.2 \times 10^5$ km (both these scale lengths are displayed as straight lines).

obtained with $l_d = 5.3 \times 10^5 R_H^{1.6}$ km. The mean value at 1 AU is almost double when the daughter scale lengths are normalized to the minimum of solar flux. Even if the daughter scale lengths are sensitive to the solar flux, changes of the latter cannot by itself explain their dispersion. Moreover, in the case of the corrected daughter scale lengths, we find a heliocentric dependence of 1.6 ± 0.2, which is in agreement with that expected from the Haser model.

2.6. Fit of the CN parent scale lengths as a function of heliocentric distance

Before we fit the parent scale length as a function of the heliocentric distance, we have tried to select some values in order to reduce the dispersion. We have searched correlations between the value of parent scale length and the value of daughter scale length which was assumed when fitting the spatial distribution, or with the activity of the comet (i.e., the gas expansion velocity). We found that no correlation and no selection could be achieved as we did for the daughter scale lengths. Thus, we have kept the complete set of 104 values of parent scale lengths.

We have fitted the parent scale length l_p as a function of the heliocentric distance R_H in a log–log plot; the same was done for the l_p values normalized to the minimum of solar flux and to 1 km s^{-1} expansion velocity. These three fits are presented in Fig. 1a–c, respectively, and results are summarized in Table 3, which also gives the correlation coefficient for each fit.

The correlation coefficients of the three fits are similar. Consequently, the corrections by the solar flux and the gas expansion velocity do not improve the fit as already noted. Our derived mean value scaled at 1 AU, and the heliocentric dependence (on original scale lengths) is in agreement with the values previously published (see Table 1). The results on the scale lengths normalized to the minimum of solar flux are similar except the mean values scaled at 1 AU, which are slightly higher. Depending on the case, we find a heliocentric dependence ranging from 1.8 to 2.1. This large value cannot be explained either by the Haser model or the model of Combi and Delsemme (1980a) (Tables 2 and 3).

3. Comparison of the production rates of CN and HCN

The quantum yield of CN production from HCN photodissociation is equal to 0.97 (Huebner et al., 1992). Because this yield is close to 1, if HCN is the only parent molecule of the CN radical, then the values of CN and HCN production rates should be close. Thus, we have compiled and compared published data in order to test the hypothesis of a single parent molecule for CN.

3.1. Compilation of the CN and HCN production rates

For CN radicals, we have chosen to compile only values that were obtained by narrow-band photometry with IHW filters, since the measurements performed by spectrophotometry with a narrow slit only view a small fraction of the coma. Therefore, among all CN production rates available in the literature, we have mainly considered the data of the team of D.G.

Table 1
Previous mean values of CN scale lengths published in the literature

Parent scale length of the CN radical in 10^3 km at 1 AU	Heliocentric dependence	Daughter scale length of the CN radical in 10^3 km at 1 AU	Heliocentric dependence	Reference
21.9 ± 0.7	1.8 ± 0.2	320		Combi and Delsemme (1980b)
12	2	300	2	Newburn and Spinrad (1984)
17	2	300	2	Cochran (1985)
16	1.5			Combi and Delsemme (1986)
18	2	420	2	Newburn and Spinrad (1989)
28 ± 14[a]	2	320^{+200}_{-100}	2	Fink et al. (1991)
23 ± 17[b]				
13	2	210	2	Randall et al. (1992), via A'Hearn et al. (1995)
54 ± 14[c]	1.3 ± 0.2			Rauer et al. (2003)
16 ± 2	1.5	300 ± 25	2	Lara et al. (2003)

[a]Average for the preperihelion period of comet Halley.
[b]Average for the postperihelion period of comet Halley.
[c]This value has been obtained from measurements on comet Hale-Bopp between 2.5 and 8 AU.

Table 2
Fits of the daughter scale lengths as a function of the heliocentric distance

	Mean value at 1 AU in 10^3 km	Heliocentric dependence	
Original scale lengths	320 ± 42	1.36 ± 0.37	$R = 0.53$
Selected original scale lengths	360 ± 34	2.02 ± 0.33	$R = 0.82$
Selected scale lengths normalized to the minimum of solar	533 ± 32	1.58 ± 0.21	$R = 0.87$

Note: The error bars are given at 1σ. R is the correlation coefficient of the fit.

Table 3
Results of the fits on the CN parent scale lengths

	Mean value at 1 AU in 10^3 km	Heliocentric dependence	
Original scale lengths	19.3 ± 1	1.86 ± 0.07	$R = 0.94$
Scale lengths normalized to the minimum of solar flux	25.3 ± 1.1	1.81 ± 0.06	$R = 0.95$
Scale lengths normalized to the minimum of solar flux and of an expansion velocity of 1 km s^{-1}	30.9 ± 1.3	2.08 ± 0.06	$R = 0.96$

Note: The error bars are given at 1σ. R is the correlation coefficient of the fit.

Schleicher and M.F. A'Hearn (see A'Hearn et al., 1995), who have published a consistent set of values for numerous comets. Indeed, it can be pointed out that production rates that have been obtained by different authors for the same comet at the same time could be different. Fink and Combi (2004) have shown that this difference is partly due to the use of different parameters to convert flux into production rates (parent and daughter scale lengths and fluorescence factors). Thus, we have gathered the observed fluxes and all the required parameters in order to perform our own consistent determination of CN production rates (heliocentric and geocentric distance, field of view and heliocentric velocity). This calculation has been made using formula (2) derived from the Haser model (O'Dell and Osterbrock, 1962; Boehnhardt et al., 1989):

$$N = \frac{Q_p}{V_{gas}} \rho \left(\frac{l_d}{l_d - l_p} \right) \left[\int_x^{\mu x} K_0(x)\,dx + \frac{1}{x}\left(1 - \frac{1}{\mu}\right) + K_1(\mu x) - K_1(x) \right], \quad (2)$$

where N is the total number of radicals within a circular aperture of radius ρ, Q_p the production rate in molecules s^{-1}, V_{gas} the expansion velocity of the gas in the coma, l_p and l_d the Haser parent and daughter scale lengths, $\mu = l_p/l_d$, $x = \rho/l_p$ and K_0 and K_1 are modified Bessel functions of the second kind of order 0 and 1. In

this calculation, we have used the values of CN scale lengths determined in Section 1 and the g-factors (fluorescence factors) from Tatum (1984) to convert measured fluxes into a number of radicals. This procedure allows us to reduce the dispersion between the CN production rate values as shown by Fink and Combi (2004) on comet 46P/Wirtanen.

Since the HCN production rates depend on the model, and especially on the assumed excitation scheme, we have chosen a consistent set of data derived from observations of numerous comets in the radio wavelengths by the Meudon team (composed of J. Crovisier, D. Bockelée-Morvan, N. Biver and coworkers). Whenever possible, we have used the re-evaluations performed by Biver (1997) with an excitation model which takes into account fluorescence as well as collisions with neutral molecules and electrons in the inner coma.

3.2. Comparison of the CN and HCN production rates for different comets

Below we present the details of our compilation for each studied comet.

3.2.1. C/1983 H1 (IRAS-Aracki-Alcock)

Bockelée-Morvan et al. (1984) have unsuccessfully searched the $J = 1-0$ HCN radio lines in this comet. They have determined a very low upper limit of 2.4×10^{25} molecules s^{-1} for the HCN production rate at 1 AU (on May 13, 1983). On the other hand, A'Hearn et al. (1983) measured a CN production rate of 5×10^{25} molecules s^{-1} on May 7, 1983. Thus, in this comet, the CN production rate is found to be at least two times greater than the HCN one. Therefore, Bockelée-Morvan et al. (1984) concluded that HCN should not be the only parent of the CN radical.

3.2.2. 21P/Giacobini-Zinner (1985 perihelion)

Bockelée-Morvan et al. (1987) have published an upper limit of 2.1×10^{25} molecules s^{-1} for the HCN production rate at $R_H = 1.03$ AU, whereas Schleicher et al. (1987) have published a CN production rate of 4×10^{25} molecules s^{-1} at the same heliocentric distance. Thus, as for IRAS-Aracki-Alcock, it seems that HCN is not the single parent of the CN radical.

3.2.3. C/1986 P1 (Wilson)

Crovisier et al. (1990) have unsuccessfully searched for HCN in this comet. When the comet was at 1.26 AU from the Sun, they have derived an upper limit for its production rate of 3×10^{25} molecules s^{-1}. At the same time, Schulz et al. (1993) have obtained narrow-band CCD images. Using a vectorial model, they have derived a production rate of about 2.3×10^{26} molecules s^{-1} at a heliocentric distance of 1.21 AU. Thus, CN production rates are 10 times larger than HCN ones. So, clearly for this comet, an additional process of CN production is required.

3.2.4. 1P/Halley

In comet Halley, HCN has always been observed through its $J = 1-0$ line and we found 22 values of HCN production rates in Bockelée-Morvan et al. (1987) and Schloerb et al. (1986) for heliocentric distances between 0.59 and 1.78 AU. At the same time, we have gathered 148 values of CN production rates for heliocentric distances between 0.67 and 2.41 AU (Schleicher et al., 1998; Catalano et al., 1986; Churyumov and Rosenbush, 1991).

Comet Halley appeared during the minimum of solar activity. In our recalculation of CN production rates (see Fig. 5), we have used our normalized CN scale lengths (i.e., $l_p = 2.5 \times 10^4 R_H^{1.8}$ km and $l_d = 5.3 \times 10^5 R_H^{1.6}$ km) and an expansion velocity of $0.85 R_H^{-0.5}$ km s^{-1} (Cochran and Schleicher, 1993).

However, even if our recalculation has reduced the dispersion, we find that the values of CN production rates, presented in Fig. 5, are still scattered. This dispersion might be due to short-term variations due to the rotation of the nucleus (Schleicher et al., 1990). This prevents us from deriving a clear conclusion from these data. But the lowest CN productions rates are approximately equal to the HCN ones, whereas the highest values are twice the HCN ones. So even if no definitive conclusion can be put forward, this suggests that the CN radical could have another source than the HCN photodissociation.

3.2.5. C/1989 X1 (Austin)

For comet Austin, six values of HCN production rates (Biver, 1997) are available for heliocentric

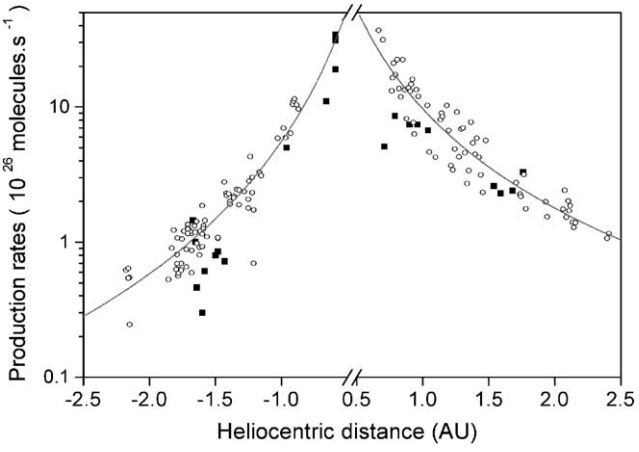

Fig. 5. CN and HCN production rates for comet 1P/Halley as a function of the heliocentric distance R_H. HCN production rates are represented as black squares and CN as open circles. The gray lines are fits by a power law of the CN production rates. To recalculate the CN production rates, we have used $l_p = 2.53 \times 10^4 R_H^{1.81}$ km, $l_d = 5.33 \times 10^5 R_H^{1.58}$ km and $V_{gas} = 0.85 R_H^{-0.5}$ km s^{-1}.

distances between 1.07 and 1.13 AU. These values are re-evaluations of those of Crovisier et al. (1993). For CN production rates, we have compiled 12 values (Waniak et al., 1994) ranging from 0.7 to 1.3 AU. All the observations were made during the postperihelion phase.

Comet Austin appeared during the maximum of solar activity; thus, for the re-evaluations of the CN production rates, we have used the scale lengths $l_p = 1.9 \times 10^4 R_H^{1.9}$ km and $l_d = 3.6 \times 10^5 R_H^2$ km (see Section 1). For the gas expansion velocity inside the coma, we have taken a value identical to the one measured on comet Halley: $0.85 R_H^{-0.5}$ km s^{-1}. HCN and CN production rates are presented as a function of the heliocentric distance in Fig. 6.

Again, HCN production rates near 1.1 AU are two times lower than the CN ones. So HCN cannot be the single parent molecules of the CN radical in comet Austin.

3.2.6. C/1990 K1 (Levy)

For comet Levy, we have found five values of HCN production rates (Biver, 1997) for heliocentric distances between 1.33 and 1.35 AU during the preperihelion phase. As for comet Austin, these values are re-evaluations of Crovisier et al. (1993). For the preperihelion phase, we found 48 values of CN production rates (Schleicher et al., 1991; Magdziarz et al., 1995). Comet Levy appeared during the maximum of the solar activity, so for the re-evaluation of CN production rates, we have used exactly the same parameters as for comet Austin. HCN and CN productions are presented as a function of the heliocentric distance in Fig. 7.

For comet Levy, HCN and CN productions are equal at a heliocentric distance of roughly 1.3 UA, suggesting that there is no additional source of CN radical.

3.2.7. C/1996 B2 (Hyakutake)

For comet Hyakutake, we have compiled 20 values of HCN production rates (Biver et al., 1999b) for heliocentric distances between 0.25 and 1.8 AU during the preperihelion phase. We can note that HCN has also been observed in the infrared near 3.3 μm (Magee-Sauer et al., 2002). The only derived production rate is about two times higher than that derived from millimeter observations at the same heliocentric distance. By Schleicher and Osip (2002) 108 values of CN production rates have been published. For the re-evaluations of the CN production rates, we have used the same values of scale lengths as for the comet Halley since comet Hyakutake appeared during the minimum of solar activity. For the expansion velocity, we have taken a value of $0.88 R_H^{-0.62}$ km s^{-1} measured in this comet (Biver et al., 1999b).

HCN and CN production rates as a function of the heliocentric distance are displayed in Fig. 8, except for the HCN production rate derived from infrared observation. Several outbursts occurred during the preperihelion phase of comet Hyakutake: a first one in March 20 (Schleicher and Osip, 2002) when the comet was at 1.16 AU from the Sun and a second one between April 13.9 and 15.7 at 0.56 AU (Biver et al., 1999b). After this second outburst, the production rates of all parent molecules (CO, H_2CO, CH_3OH, CS) have decreased. This fact is also true for HCN as seen in Fig. 8. The trend of the production rates in the

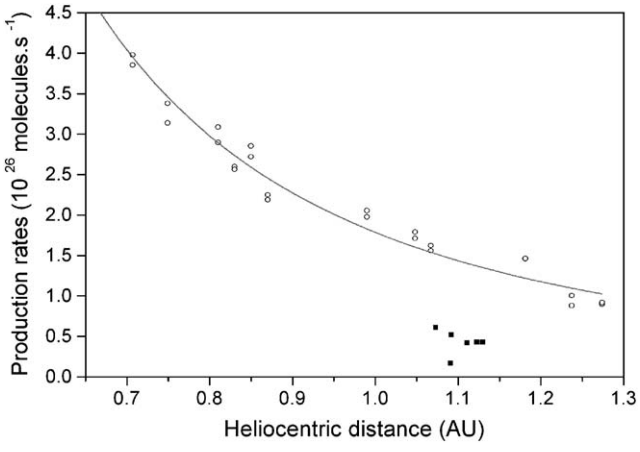

Fig. 6. CN and HCN production rates for comet C/1989 X1 (Austin) as a function of the heliocentric distance R_H. HCN production rates are represented as black squares and CN as open circles. The gray line is a fit by a power law of the CN production rates. To recalculate the CN production rates, we have used $l_p = 1.93 \times 10^4 R_H^{1.86}$ km, $l_d = 3.6 \times 10^5 R_H^{2.02}$ km and $V_{gas} = 0.85 R_H^{-0.5}$ km s^{-1}.

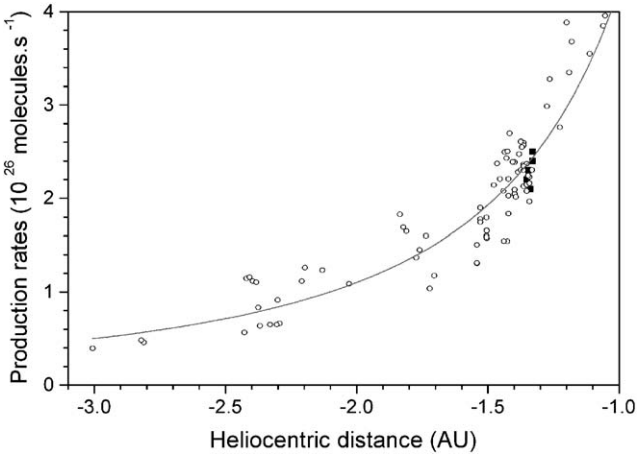

Fig. 7. CN and HCN production rates for comet C/1990 K1 (Levy) as a function of the heliocentric distance R_H. HCN production rates are represented as black squares and CN as open circles. The gray line is a fit by a power law of the CN production rates. To recalculate the CN production rates, we have used $l_p = 1.93 \times 10^4 R_H^{1.86}$ km, $l_d = 3.6 \times 10^5 R_H^{2.02}$ km and $V_{gas} = 0.85 R_H^{-0.5}$ km s^{-1}.

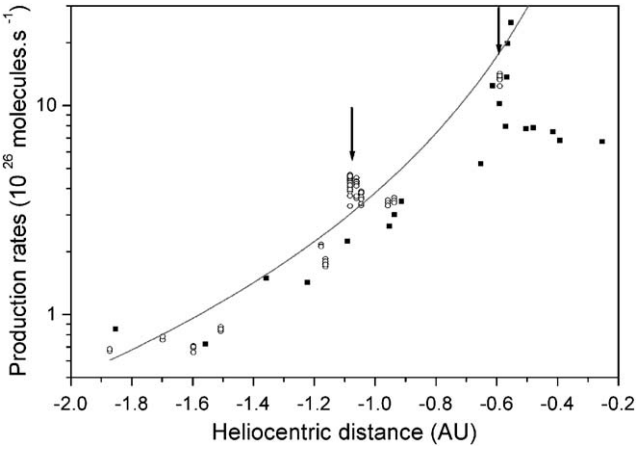

Fig. 8. CN and HCN production rates for comet C/1996 B2 (Hyakutake) as a function of the heliocentric distance R_H. HCN production rates are represented as black squares and CN as open circles. The gray line is a fit by a power law of the CN production rates. The arrows represent the location of both outbursts. To recalculate the CN production rates, we have used $l_p = 2.53 \times 10^4 R_H^{1.81}$ km, $l_d = 5.33 \times 10^5 R_H^{1.58}$ km and $V_{gas} = 0.88 R_H^{-0.63}$ km s^{-1}.

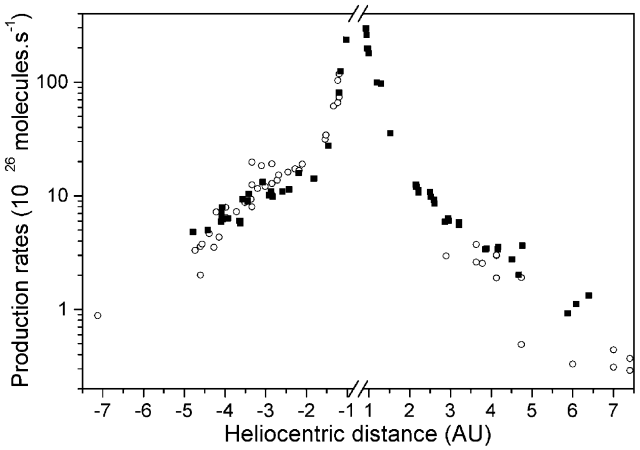

Fig. 9. CN and HCN production rates for comet C/1995 O1 (Hale-Bopp) as a function of the heliocentric distance R_H. HCN production rates are represented as black squares and CN as open circles.

preperihelion phase of comet Hyakutake is complex. Thus, it prevents us from giving a clear conclusion. However, one can note that for all the heliocentric distances, the HCN and CN production rates are approximately equal.

3.2.8. C/1995 O1 (Hale-Bopp)

For comet Hale-Bopp, we have gathered 49 values of HCN production rates (Biver, 1997; Biver et al., 1999a, 2002) for heliocentric distances between 0.92 and 6.39 AU. As for comet C/1996 B2 Hyakutake, HCN has also been observed in the infrared; the derived production rates are about two times higher than those derived from millimeter observations (Magee-Sauer et al., 1999). For the CN production rates, we have compiled 52 values (Rauer et al., 2003; Schleicher et al., 1997). Since flux values have not been published, we were not able to re-evaluate the CN production rates as we did for the previous comets. However, we have modified the values of Schleicher et al. (1997) using the velocity dependence of Biver et al. (1999a). We have chosen the values of Rauer et al. (2003) despite the fact that they have been obtained from spectrophotometry (no observations by narrow-band photometry have been published for heliocentric distances greater than 3 AU). Moreover, Rauer et al. (2003) have already made this comparison between HCN and CN production rates (see their Fig. 9) for comet Hale-Bopp. Our compilation is presented in Fig. 9. We have not represented the values of HCN production rates derived from infrared observations, as they extend to a very small range of heliocentric distances. Like Rauer et al. (2003), we conclude that the production rates of the two species are approximately equal for the whole range of heliocentric distances.

3.3. Discussion

The production rates are model dependent. The CN radical production rates depend on the g-factors and on the daughter and parent scale lengths, so we have studied the sensibility of each of these parameters on the resulting CN production rates. This study has been undertaken on the CN production rates that we have compiled on comet 1P/Halley since the details of the observations are available on a large range of heliocentric distances. The results are as follows:

1. If we use the g-factors of Schleicher et al. (1998) rather than those of Tatum (1984), the CN production rates increase up to 27%. Indeed, the g-factors of Schleicher et al. (1998) are slightly lower than those of Tatum (1984); then from the same value of flux, they lead to a greater number of radicals present in the field of view and then to a greater production rate.
2. If the daughter scale length is increased from $2.1 \times 10^5 R_H^{1.4}$ to $4.2 \times 10^5 R_H^{1.4}$ km (extreme values which have been published so far, see Table 1), the CN production rate decreases by 25%.
3. If the parent scale length is increased from $1.2 \times 10^4 R_H^{1.8}$ to $2.8 \times 10^4 R_H^{1.8}$ km (extreme values for heliocentric distances lower than 3 AU which have been published so far, see Table 1), the CN production rate increases by 93%.

This clearly shows that the most sensitive parameter for the calculation of the CN production rate with a Haser model is the parent scale length. Moreover, if one

considers all these parameters in the range of the previously published values, the resulting CN production rates vary as much as a factor of 2 as already noted by Fink and Combi (2004). These variations of CN production rates as a function of the values of parent and daughter scale lengths are illustrated in Fig. 10a and b. These figures present the minimal and maximal values which could be derived for comets Halley and Austin.

Comet Austin is an example for which the CN production rates are clearly higher than the HCN ones, whatever the values of scale lengths used (Fig. 10b). Then, for this comet, it is clear that at least half of CN radicals come from another source than the HCN photolysis. Comets IRAS-Aracki-Alcock, Giacobini-Zinner and Wilson also show higher CN production rates than the HCN ones, considering that only upper limits of HCN production rates have been published. In comet Halley, it seems that the CN ones are slightly higher than the HCN ones, when the comet is closer than 1.5 AU to the Sun. But comets Hale-Bopp, Levy and Hyakutake exhibit similar CN and HCN production rates.

In conclusion, whereas CN radicals could be almost entirely produced by HCN photolysis in some comets, an additional process of CN production is required in other ones.

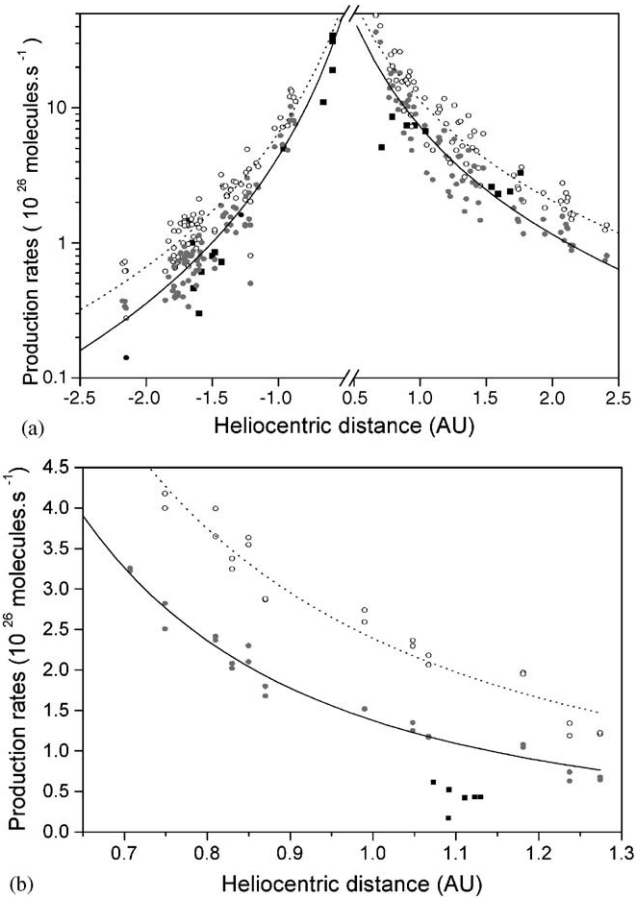

Fig. 10. (a) Sensitivity of the CN production rates of comet 1P/Halley to the values of the parent and daughter scale lengths. The open circles are the maximal CN production rates calculated with $l_p = 2.8 \times 10^4$ km and $l_d = 2.1 \times 10^5$ km, and the solid circles are the minimal values of CN production rates (calculated with $l_p = 1.2 \times 10^4$ km and $l_d = 5.3 \times 10^5$ km). The HCN production rates have also been displayed as black squares for comparison. (b) Similar to (a), but for comet C/1989 X1 (Austin).

4. Comparison of photochemical data of some CN-bearing molecules with the CN parent scale length

Since the origin of CN is difficult to constrain by the comparison between HCN and CN production rates alone, we have compared the CN parent scale length with the photodissociation rate of the possible gaseous parent molecules. After HCN, which is the major parent molecule, we have considered some others CN-bearing molecules, CH_3CN, HC_3N and HNC, that have already been detected in cometary atmospheres (Bockelée-Morvan et al., 1999) and also C_2N_2 and C_4N_2 that have been proposed as CN parent molecules (Festou et al., 1998; Krasnopolsky, 1991). Among the detected CN-bearing molecules (Bockelée-Morvan et al., 1999):

- HC_3N and CH_3CN have production rates about 1/10 that of HCN.
- HNC is observed with an HNC/HCN varying from 0.03 to 0.2, depending on the comet and on the heliocentric distance.

Thus, HCN is by far the most important progenitor for CN.

4.1. Model of Combi and Delsemme (1980a)

The photodissociation rate cannot be directly compared to the CN parent scale length determined by a Haser model. Since during the photodissociation process, the radical can receive an excess of energy and be released from the parent molecule in any direction, the Haser radial scale lengths have no immediate physical meaning and cannot be directly compared to the ratio of the expansion velocity to the photodissociation rate. Therefore, we have used the model of Combi and Delsemme (1980a) in order to compare the photodissociation rate to the CN parent scale length.

Using an average random walk model, Combi and Delsemme (1980a) have shown that, when the daughter scale length is much larger than the parent molecule one, which is the case for CN, the actual parent scale length

(defined as $l_p = V_{gas}/\beta_p$) and the observed Haser scale length l_{pH} are related by the simple formulae

$$l_{pH} = l_p \sin\delta \quad \text{with} \quad \tan\delta = V_{gas}/V_e, \tag{3}$$

where V_{gas} is the expansion velocity of the parent molecule, V_e the ejection velocity of the radical and β_p the photodissociation rate of the parent molecule. Finally, we have

$$l_{pH} = \frac{1}{\beta_p}\frac{V_{gas}^2}{[V_{gas}^2 + V_e^2]^{1/2}}. \tag{4}$$

This formula is valid if the quantum yield of CN production is equal to one. If it is not the case, we have to multiply the photodissociation rate of the parent molecule by the quantum yield of CN production. We call the scale lengths calculated with formula (4) "effective Haser scale length".

4.2. Photochemical data of the possible gaseous parent of the CN radical

In this section, we present the photodissociation properties of the possible gaseous parent molecules of the CN radical (HCN, CH_3CN, HC_3N, HNC, C_2N_2 and C_4N_2).

4.2.1. Hydrogen cyanide (or HCN)

HCN is mainly photodissociated by vacuum ultraviolet radiations into CN radical with a quantum yield equal to 0.97 (Huebner et al., 1992). In the solar radiation field, the published values of photodissociation rates at 1 AU and quiet Sun conditions range from 1.1×10^{-5} to $1.51\times10^{-5}\,s^{-1}$ (see Table 4), with a major contribution from Lyman α (122 nm). In this paper, we use a mean value of $1.3\times10^{-5}\,s^{-1}$. Jackson (1991) claimed that at this energy, CN radicals are produced in the $B^2\Sigma^+$, $A^2\Pi_I$ and $X^2\Sigma^+$ states. The excess velocity for these three different states has been calculated by Bockelée-Morvan and Crovisier (1985) (see Table 4). But more recent studies at 122 nm have shown that the CN radical is mainly produced in the $A^2\Pi_I$ state (Morley et al., 1992; Cook et al., 2000). At 157 nm, the available energy for disposal in the H and CN fragments is 1.32 ± 0.02 eV and the rotationnal and vibrationnal energies represent 25% of the excess energy (Guo et al., 2000). Hence, we can estimate that at Lyman α the excess energy, which could be converted into kinetic energy, is 2.72 eV. Using the conservation of energy and momentum, we can evaluate that CN radicals will have an excess velocity $V_{eHCN} = 0.864\pm0.006\,km\,s^{-1}$. This new value of the ejection velocity of the CN radical gives strong constraints on the comparison between the CN parent scale length and the photodissociation rate of HCN (see Section 4.3).

4.2.2. Methyl cyanide (or CH_3CN)

Bockelée-Morvan and Crovisier (1985) have calculated the photodestruction rate of CH_3CN in cometary conditions to be of $6.68\times10^{-6}\,s^{-1}$. But Halpern (1987) and Kanda et al. (1999) have shown that the CN production is a minor channel in the photodissociation of CH_3CN in the VUV region. The dominant pathway being the H elimination, the quantum yields of CN production could be lower than 0.02 (Kanda et al., 1999). Thus, the production rate of CN from CH_3CN photodissociation could be 100 times lower than that of HCN, with a value of about $10^{-7}\,s^{-1}$.

4.2.3. Cyanoacetylene (or HC_3N)

Considering that the CN production quantum yield is equal to 1, numerous values of HC_3N photodestruction rates have been published ranging from 2.8×10^{-5} to $7.7\times10^{-5}\,s^{-1}$ (see Table 4). The higher values take into account the electronic transition $^1\Delta - {}^1\Sigma_g$ (Bruston et al., 1989) around 190–230 nm (Crovisier, 1994). Then, at a first glance, those values seem to be more reliable for the total photodestruction rate of this molecule. But, the threshold for the CN production has been determined to be 185–200 nm (Clarke and Ferris, 1995). Thus, the lowest values of the HC_3N photodissociation rate should better correspond to the CN production rate from HC_3N photolysis. Hence, in the remainder of this article, we use a photodissociation rate of $3.4\times10^{-5}\,s^{-1}$ (Krasnopolsky, 1991). Furthermore, the quantum yield of CN production rate has never been directly measured in the VUV and Halpern et al. (1988) suggest that this quantum yield could be as low as 0.05 at 193 nm.

4.2.4. Cyanogen (or C_2N_2)

Jackson (1976) and Bockelée-Morvan and Crovisier (1985) have calculated the photodissociation rate of C_2N_2 (see Table 4) in cometary conditions. Both values are very different (9.1×10^{-5} and $3.08\times10^{-5}\,s^{-1}$). The quantum yield of CN production is also uncertain. Bockelée-Morvan and Crovisier (1985) proposed a value of 2, whereas Yung et al. (1984) used a value of 0.6. The state in which CN is formed is also not very well defined, but at 122 nm it could be produced in the $B^2\Sigma^+$ and $X^2\Sigma^+$ states (Bockelée-Morvan and Crovisier, 1985). In this case, the ejection velocity should be approximately equal to $2.07\,km\,s^{-1}$ for each radical (Bockelée-Morvan and Crovisier, 1985) (see Table 4).

4.2.5. Dicyanoacetylene (or C_4N_2)

Krasnopolsky (1991) has investigated the possibility that C_4N_2 could be a parent of the CN radicals and calculated its photodissociation rate. Depending on hypothesis on the threshold of CN production, the photodissociation rate of C_4N_2 range from 5×10^{-5} to $1.5\times10^{-4}\,s^{-1}$ (see Table 4).

Table 4
Photodissociation data of HCN, CH_3CN, HC_3N, C_2N_2 and C_4N_2

Molecules	Photodissociation rate (s^{-1})	Excess energy (eV)	Ejection velocity ($km\,s^{-1}$)	Remarks	References
HCN	1.3×10^{-5}				Huebner and Carpenter (1979)
	1.1×10^{-5}	3.8	1.02	$HCN\rightarrow H+CN(A^2\Pi_I)$	Combi and Delsemme (1980b)
				CN is formed in the state	
	1.51×10^{-5}	2.01	0.74	$B^2\Sigma^+$	Bockelée-Morvan and Crovisier
		4.08	1.06	$A^2\Pi_I$	(1985)
		5.21	1.19	$X^2\Sigma^+$	
	1.26×10^{-5}	3.82		$HCN\rightarrow H+CN(A^2\Pi_I)$	Huebner et al. (1992)
	4.51×10^{-7}	11.2		$HCN\rightarrow HCN^++e^-$	
		2.72	0.864	$HCN\rightarrow H+CN(A^2\Pi_I)$	This work
CH_3CN				CN is formed in the state	
	6.68×10^{-6}	2.56	2.63	$B^2\Sigma^+$	Bockelée-Morvan and Crovisier
		4.63	3.53	$A^2\Pi_i$	(1985)
		5.76	3.94	$X^2\Sigma^+$	
HC_3N	7.7×10^{-5}				Jackson (1976)
	2.8×10^{-5}				Huebner and Carpenter (1979)
				CN is formed in the state	
		0.79	1.69	$B^2\Sigma^+$	Bockelée-Morvan and Crovisier
		2.86	3.21	$A^2\Pi_i$	(1985)
		3.99	3.80	$X^2\Sigma^+$	
	3.4×10^{-5}		2.5 ± 0.5		Krasnopolsky (1991)
	3.92×10^{-5}	2.65			Huebner et al. (1992)
	6.6×10^{-5}				Crovisier (1994)
C_2N_2	9.1×10^{-5}				Jackson (1976)
	3.08×10^{-5}	1.16	2.07	$CN\ (X^2\Sigma^+)+CN\ (B^2\Sigma^+)$	Bockelée-Morvan and Crovisier
		2.10	2.78	$2\ CN\ (A^2\Pi_I)$	(1985)
		4.36	3.96	$2\ CN\ (X^2\Sigma^+)$	
	3×10^{-5}		2.5 ± 0.5		Krasnopolsky (1991)
C_4N_2	5×10^{-5}		3	For $\lambda<196$ nm	Krasnopolsky (1991)
	1.5×10^{-4}		1.5	For $\lambda<232$ nm	Krasnopolsky (1991)

4.2.6. *Hydrogen isocyanide (or HNC)*

No photodissociation rate in the solar radiation field has been reported for HNC. Millar et al. (1991) assume that the photodissociation rate of HNC is equal to the HCN one found in the ISM. So we have considered a photodissociation rate of HNC equal to the HCN one in the solar radiation field, i.e., $1.3\times10^{-5}\,s^{-1}$.

4.3. *Comparison of the CN parent scale length with the HCN photodissociation rate*

In order to compare the observed CN parent scale length to the photochemical data of HCN given for the minimum of solar activity, we have taken as a reference value the scale lengths that we have normalized to the minimum of solar flux. We have used Combi and Delsemme's model (1980a) in order to calculate the CN parent scale length from the HCN photodissociation rate. The results of this comparison are presented in Fig. 11. For this calculation, we have chosen a heliocentric dependence of the expansion velocity of $R_H^{-0.42}$ as measured in comet C/1995 O1 (Hale-Bopp) (Biver et al., 2002) and an averaged value of HCN photodissociation rate of $1.3\times10^{-5}\,s^{-1}$.

As one can see in Fig. 11, if one considers only HCN as a parent of the CN radical, the heliocentric evolution of the CN parent scale lengths is not well reproduced, except for $R_H>3$ AU, where the measured CN parent scale lengths are in agreement with the predicted ones. This is consistent with the observation of almost equal HCN and CN production rates for this range of heliocentric distances in comet C/1995 O1 (Hale-Bopp) (Rauer et al., 2003). For heliocentric distances lower than 3 AU, the measured CN parent scale lengths are shorter than the predicted ones. Indeed, the calculated effective HCN scale length at 1 UA is $5.8^{+3.0}_{-1.8}\times10^4$ km at 1 UA, whereas the observed CN parent one is about $2.5^{+2.5}_{-1.5}\times10^4$ km. This discrepancy could be explained in part by the acceleration of the gas in the inner coma (see Section 6). Nevertheless, the HCN photodissociation alone cannot explain the spatial distribution of CN for this range of heliocentric distances and an additional

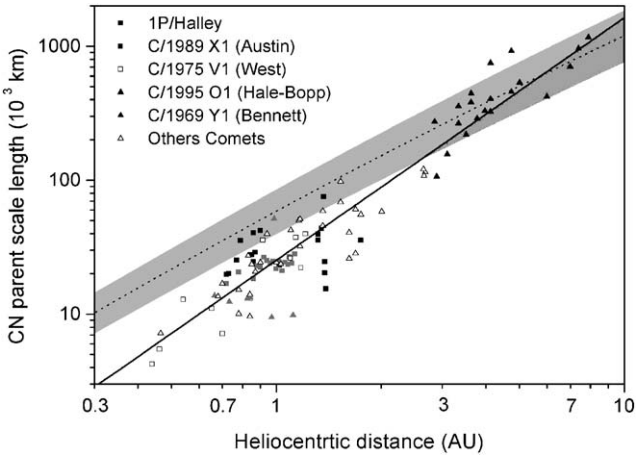

Fig. 11. Measured and effective CN parent scale lengths as a function of the heliocentric distance R_H. The points are the CN parent scale lengths normalized to the minimum of solar flux (see Section 1). The black line is the best fit ($2.53 \times 10^4 R_H^{1.81}$ km). The dashed line is the effective CN parent scale length with $\beta = 1.3 \times 10^{-5}\,s^{-1}$, $V_{gas} = 1R_H^{-0.42}\,km\,s^{-1}$ and $V_e = 0.864\,km\,s^{-1}$. The gray region represents the error on the effective CN parent scale lengths due to uncertainties on the photodissociation rate of HCN ($\pm 0.2 \times 10^{-5}\,s^{-1}$) and on the expansion velocity ($\pm 0.15\,km\,s^{-1}$). The heliocentric dependence of the expansion velocity $R_H^{-0.42}$ is from Biver et al. (2002).

parent is required, at least in some comets. The effective Haser scale length of this additional parent has to be smaller than 2.5×10^4 km at 1 AU.

4.4. Comparison of the CN parent scale length with the photochemical data of CH_3CN, HC_3N, HNC, C_2N_2 and C_4N_2

If another gaseous molecule could explain the difference between the measured and the effective Haser scale lengths from HCN photodissociation, its photodissociation rate has to be higher than the HCN one. This excludes CH_3CN and HNC, for which photodissociation rates are very close or lower than the HCN's one.

The case of HC_3N is more ambiguous. The absorption of one photon could produce the CN radical. But with a photodissociation rate of $3.4 \times 10^{-5}\,s^{-1}$ (Krasnopolsky, 1991), a CN quantum yield of production equal to 1, an ejection velocity of $2.5\,km\,s^{-1}$ (Krasnopolsky, 1991) and an expansion velocity of $1\,km\,s^{-1}$, the effective CN parent scale length could be about 1.1×10^4 km, i.e., shorter than the HCN one. So HC_3N could act as a second parent of the CN radicals as proposed by Krasnopolsky (1991). If we suppose that the CN profile is correctly modeled by a Haser profile with $l_p = 2.5 \times 10^4$ km, $l_d = 5.3 \times 10^5$ km and $V_{gas} = 1\,km\,s^{-1}$, that the photodissociation rate of HC_3N is about $3.4 \times 10^{-5}\,s^{-1}$ and that the quantum yield of CN production from HC_3N photolysis is equal to 1, then the HC_3N production rate has to be between 20% (for $\beta_{HCN} = 1.51 \times 10^{-5}\,s^{-1}$, $V_{eHCN} = 0.864\,km\,s^{-1}$ and $V_{eHC3N} = 4\,km\,s^{-1}$) and 70% (for $\beta_{HCN} = 1.1 \times 10^{-5}\,s^{-1}$, $V_{eHCN} = 0.864\,km\,s^{-1}$ and $V_{eHC3N} = 2\,km\,s^{-1}$) of the HCN one. These abundances are higher than the observed HC_3N production rate, which is only 10% of the HCN one (Bockelée-Morvan et al., 1999). Further experimental studies on the HC_3N photodissociation are needed to constraint the role of this compound in the origin of the cometary CN radical.

C_2N_2 was proposed as a parent molecule for the CN radicals by Bockelée-Morvan and Crovisier (1985) and Festou et al. (1998). We have calculated the effective CN parent Haser scale lengths for this molecule using a quantum yield of CN production equal to 2 (Bockelée-Morvan and Crovisier, 1985; Halpern and Yuhuia, 1997) and a photodissociation rate equal to $\beta = 3.1 \times 10^{-5}\,s^{-1}$ (Bockelée-Morvan and Crovisier, 1985; Krasnopolsky, 1991). In Fig. 12, we present the effective CN parent scale lengths from C_2N_2 photodissociation as a function of the ejection velocity at 1 AU and for three different expansion velocities. All the calculated Haser scale lengths are shorter than the measured one. Thus, a mixture of HCN and C_2N_2 could explain the observed radial profile of the CN radical. Then, we have calculated the fractions of CN radical which have to be produced from C_2N_2 and HCN photodissociation in order to reproduce a radial profile of CN. As for the study of HC_3N, we have supposed that the CN profiles are correctly modeled by a Haser profile with $l_p = 2.5 \times 10^4$ km, $l_d = 5.3 \times 10^5$ km and $V_{gas} = 1\,km\,s^{-1}$. We have found that the ratio of the C_2N_2 production rate to the HCN one has to be between 25% and 85%. Unfortunately, C_2N_2 has never been detected in comets and no upper limits have been published. The reason is that this molecule has no

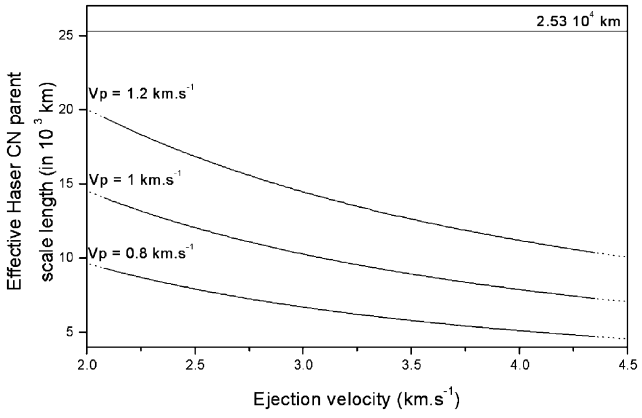

Fig. 12. Effective CN parent scale lengths from C_2N_2 photodissociation as a function of the ejection velocity of the CN radical (photodissociation rate $\beta = 3.1 \times 10^{-5}\,s^{-1}$). The three curves correspond to three different expansion velocities and the horizontal line represents the mean value of the CN parent scale lengths measured in comets and scaled to the minimum of the solar flux.

allowed rotational transitions, and its low vibrational band strengths do not lead to favorable excitation conditions in the infrared (Crovisier, 1987). In the same conditions and especially for the same production rate, the C_2N_2 vibrational band at 2157 cm^{-1} is 25 times less intense than the CO vibrational band at 2143 cm^{-1} (Crovisier, 1987). C_2N_2 is then almost undetectable in the 5 μm window. Despite the fact that C_2N_2 also has a vibrational band at 233 cm^{-1} (43 μm), it remains impossible to detect it by ground-based observations. Thus, even if the production rate of C_2N_2 is comparable to HCN one, this specie is quite difficult to detect by remote sensing. Indirect methods have been proposed by Petrie et al. (2003) consisting in trying to detect the $NCCNH^+$ ion or the polar isomer NCNC. As a matter of fact, C_2N_2 has never been detected in laboratory cometary ice analogs (Cottin et al., 1999), so its presence in comets has yet to be proven. The only astrophysical environment where this molecule has been detected is Titan's atmosphere in which it is produced by a specific chemistry dominated by N_2 and CH_4. The case for C_4N_2 is very similar to that for C_2N_2 except that its photochemistry is very badly known.

5. Observations of gaseous jets

Since the discovery of the CN jets in comet Halley by A'Hearn et al. (1986a), it has been proposed that the CN seen in the jets could be produced by the submicronic CHON grains discovered by Kissel et al. (1986). This hypothesis was proposed because no counterpart of this CN emission was visible in nearly simultaneous images taken in the diffused continuum (A'Hearn et al., 1986a).

In comet Halley, some C_2, C_3, OH and NH jets have also been detected and they have the same features as the CN jets (Cosmovici et al., 1988; Clairemidi et al., 1990a, b). Dust jets have also been observed, but it is not clear whether they are coincident or not with the gaseous jets. On the one hand, A'Hearn et al. (1986b) mentioned that the jets do not exist in the continuum images although it appears that one of the CN jets may come from the same area on the nucleus that produces most of the dust. On the other hand, the dust jets seen with the UV spectrometer of Vega 2 are co-spatial with all the gas jets (Goidet-Devel et al., 1997).

In comet Hale-Bopp, CN, C_2, C_3, OH and NH jets have also been observed (Lederer et al., 1999). This observation confirms the detection of CN jets by Larson et al. (1997) and Mueller et al. (1999). Near the perihelion, the CN images show a spiral pattern while the continuum shows some arcs confined to the sunward side (Mueller et al., 1999; Lederer et al., 1999). In these observations, dust jets coincided with the CN jets in the sunward direction, but not in the anti-sunward direction (Lederer and Campins, 2002).

Clairemidi et al. (1990a) have studied the radial intensity of a CN jet in comparison to a diffuse component (where no jets are present) called "valley". The CN spatial distributions in the jets and in the valley are quite similar up to 8000 km, but do not match anymore beyond this. It seems necessary to introduce a local production mechanism inside the jets to explain such a behavior. Klavetter and A'Hearn (1994) have performed a similar study. They have clearly shown that the CN radial profile of the diffuse component is different from that inside the jet. On the one hand, the profile of the diffuse component can be fitted with Haser or vectorial models, and thus is consistent with a simple photodissociation process. On the other hand, the jet profile cannot be explained by some simple process. Thus, using a numerical derivative of the profile, Klavetter and A'Hearn (1994) found that the CN production inside the jet occurs up to 15,000 km with a maximum approximately at 8000 km. This shift of the production peak from the nucleus to the coma is by definition an extended source. Klavetter and A'Hearn (1994) proposed that the CN is released from grains, the temperature of which increases with time, and therefore produce CN faster. Lederer and Campins (2002) have modeled the CN jets observed on comet Hale-Bopp with a 3-D time-dependent Monte-Carlo model considering that the daughter radicals are produced by photodissociation of parent gas and by an extended source. With this model, they have correctly reproduced the appearance of the CN jets, and also those of C_2 and OH. In one jet, 75% of the CN radicals seem to be produced by an extended source (Lederer and Campins, 2001).

From these three studies, we see that a large fraction of the CN that is present in the jets seems to be produced by an extended source whose productivity does not peak at the nucleus. Similar results have been obtained by Eberhardt et al. (1987) for the in situ measurements of CO by the Giotto neutral mass spectrometer (NMS). The measured density profile can only be explained if the CO production is maximum at 9000 km from the nucleus. The additional process cannot be the photodissociation of a gaseous parent, otherwise the peak production would be located at the nucleus surface where the density of the parent is maximal. The displacement of the production peak should rather be due to chemical reactions in the inner coma, release of gaseous parents during the fragmentation of grains, sublimation of icy grains or thermal degradation of large compounds present on grains. This will be discussed in Section 6.

6. Summary and discussion

We have compared CN and HCN production rates for eight comets (see Section 3). For four of them

(Austin, IRAS-Aracki-Alcock, Giacobini-Zinner and Wilson), the CN production rates are significantly higher than those of HCN. This leads to the conclusion that CN radicals cannot be produced only by the HCN photolysis and that an additional process is required. For comets Halley, Levy, Hyakutake and Hale-Bopp, CN and HCN production rates are quite similar. But for all comets, the CN parent scale lengths are lower than the scale length predicted from HCN photolysis for $R_H < 3$ UA, as we showed in Section 4. This fact has already been noted by Lara et al. (2003). But this result has to be taken with caution since the CN production rates are only known with a factor of 2 when taking into account all uncertainties (see Fig. 10a and b).

In order to convert the measured flux into CN production rates, one needs to know the parent scale length, which is the most sensitive parameter for this calculation. Since the CN parent scale lengths are lower than those corresponding to HCN photolysis and since production rates increase with parent scale lengths, the use of the effective scale length of HCN photodissociation leads to CN productions that are two times larger than the HCN production for all comets. Thus, only a fraction of CN radicals are effectively produced by the HCN photolysis and CN production rates should be calculated only with a model that takes into account the additional CN production mechanisms.

In Section 2, we have presented a compilation of the available parent and daughter CN Haser scale lengths. These CN Haser scale lengths present a large dispersion. We have shown that this dispersion is not due to the change of solar flux or variation of the gas expansion velocity from one comet to another. This dispersion derived certainly from the fact that most spatial measurements yield to a set of satisfying solutions: several parent and daughter scale length pairs lead to good fits between the Haser model and the spatial data. In order to correctly extract both parent and daughter scales lengths, the spatial distribution of CN has to extend far enough from the nucleus. Otherwise the CN daughter scale length (and consequently the parent scale length) cannot be adequately measured. Therefore, observations with a wide field of view telescope are necessary to constrain correctly the CN Haser scale lengths. We have also pointed out that short-term variations of the CN production rate, related to the rotation of the nucleus, could also be responsible in part for the dispersion observed in the values of CN Haser scale lengths, since the Haser model supposes a steady-state production rate.

Despite the dispersion of the CN Haser parent scale lengths, we have compared them with the photodissociation rate of HCN using the model of Combi and Delsemme (1980a) (Fig. 11). When the comet is located at heliocentric distances larger than 3 UA, the CN spatial distribution is consistent with HCN photolysis. Then, at these heliocentric distances, the CN radical could be entirely produced by HCN photodissociation as already shown by Rauer et al. (2003). Nevertheless, for heliocentric distances lower than 3 AU, the observed CN parent scale lengths are shorter than the predicted ones, as already shown by Bockelée-Morvan and Crovisier (1985), Krasnopolsky et al. (1991) and Lara et al. (2003). At 1 AU, the equivalent CN Haser scale length from HCN photolysis is equal to 5.9×10^4 km whereas the mean value of the observed ones is 2.5×10^4 km; then the spatial distribution of CN could not be explained so far by HCN photolysis alone. The acceleration of the gas in the inner coma could partly explain this difference. Indeed, between 10^2 and 10^4 km from the nucleus, the gas expansion velocity increases by a factor roughly equal to 1.5 (Combi, 1989; Combi et al., 1997). Whereas this factor could be higher in very productive comets such as C/1995 O1 (Hale-Bopp), it seems to be smaller than the ratio between the predicted and observed CN parent scale lengths. Surely, this acceleration could not fully explain this discrepancy. Nevertheless, no modeling of this effect on the CN spatial distribution has ever been performed so far.

To explain the discrepancy between the observed and predicted CN Haser parent scale lengths, another hypothesis can also be put forward: the presence of another CN production mechanism than HCN photolysis. This interpretation is supported by the observation of CN jets and particularly by the CN radial distribution inside jets which are not consistent with a production from a simple photodissociation process (Klavetter and A'Hearn, 1994). Moreover, from observations of CN in several comets, Arpigny et al. (2003), Jehin et al. (2004) and Manfroid et al. (2005) have derived an anomalously low $^{14}N/^{15}N$ isotopic ratio (about 130, compared with the terrestrial ratio of 280). This is quite different from $^{14}N/^{15}N$ isotopic ratio determined from the radio lines of HCN observed in comet Hale-Bopp, which is, in that case, close to the terrestrial ratio (Jewitt et al., 1997). This strongly suggests another source of CN, significantly enriched in ^{15}N as compared to HCN. Thus, HCN cannot be the unique source of CN radicals in comets. The different hypotheses for this additional source of cometary CN radicals are detailed below.

First, the CN spatial distribution could be explained by the photodissociation of another parent(s) molecule(s). In Section 4, we have studied the possible additional parents: CH_3CN, HNC, HC_3N, C_2N_2 and C_4N_2. CH_3CN and HNC, whose scale lengths are larger or of the same order than the one determined for CN parents, could not act as the second parent of the CN radical. HC_3N and C_2N_2 scale lengths could be consistent with the observed CN spatial profiles. The photodissociation of HC_3N, and particularly the quantum yields of CN production in cometary conditions, is not well known. Nevertheless, even if we suppose a

quantum yield of 1, the required production rate of HC_3N in order to explain the CN density profile would be higher than the measured one (Bockelée-Morvan et al., 1999). Thus, it seems improbable that HC_3N could explain the CN density profile. C_2N_2 has been proposed (Bockelée-Morvan and Crovisier, 1985; Festou et al., 1998) since its photodissociation leads to an effective scale length lower than the one measured for the CN parent (see Fig. 12). Unfortunately, C_2N_2 has no allowed rotational transition and its vibrational band strengths are very low (see Section 4); this leads to a very high detection limit for this compound. The hypothesis of this compound as a parent of the CN radical cannot be ruled out, but it will be hard to confirm since its detection is a very challenging issue.

Another possible mechanism is the production of CN radical by chemical reactions. Rodgers and Charnley (1998) have invoked such a process to explain the HNC extended source in comet Hale-Bopp. But it has been demonstrated that this process is not efficient enough to explain the HNC production in less productive comets such as Hyakutake or Lee (Rodgers and Charnley, 2001). It might also be the case for CN. But in order to confirm this statement, a specific model of CN production by chemical reactions has to be developed.

Finally, a mechanism where CN radical is produced directly from dust has been proposed by numerous authors. Such a mechanism was originally put forward to explain the presence of CN jets (A'Hearn et al., 1986a), since CN spatial profile inside the jets cannot be explained by the photodissociation of a gaseous molecule (Klavetter and A'Hearn, 1994). A'Hearn et al. (1995) and Newburn and Spinrad (1989) noticed that there is a correlation between the CN and dust production rates. Cottin et al. (2004) have recently demonstrated that H_2CO could be produced by the thermal degradation of polyoxymethylene (H_2CO polymer). This mechanism could then be responsible for the H_2CO extended source. A similar mechanism could be at the origin of the CN spatial distribution. Unfortunately, the model of Cottin et al. (2004) is, so far, not applicable to the CN extended source, because of the lack of chemical data concerning the degradation of high molecular weight nitrogenated compounds that could be present on cometary grains. Consequently, experimental studies on the measurements of CN production by heating and UV irradiation of nitrogenated compounds, such as HCN polymers or hexamethylenetetramine ($C_6H_{12}N_4$), have to be performed.

7. Conclusion

HCN photolysis is the major process in the production of CN in cometary atmospheres, but it cannot entirely explain the CN density profile and the CN production rates in most comets. Moreover, even if in some comets, the Haser CN production rates seem to be in agreement with those of HCN, the CN density profile can never be explained by HCN photolysis alone when the comet is closer than 3 AU from the Sun. The acceleration of gas in the inner coma could play a role, but further modeling of this effect is required. As a matter of fact, an additional production of CN is necessary to explain the spatial profile of CN inside the jets as well as the discrepancy between the $^{14}N/^{15}N$ isotopic ratio measured in CN and HCN.

A part of CN radicals could also be formed by HC_3N or C_2N_2 photolysis. But, even if the production of CN radicals from the HC_3N photolysis is poorly documented, HC_3N production rate seems to be too low to explain quantitatively the CN density profile. C_2N_2 is also a candidate to be the second parent of CN radicals. Unfortunately, no upper limit for its production rate has been published due to its difficult detection from ground-based observations. A challenging issue will be its in situ measurements by the Rosetta spacecraft or observations from space in the far infrared. Additionally, to get a better idea of the role of HC_3N and C_2N_2, further experimental studies of their photolysis should be performed, mainly at 121.6 nm (Lyman α).

At last, the hypothesis of the production of CN radical by photo- or thermal degradation of high molecular weight nitrogenated compounds present on cometary grains has to be explored. Modeling of this process should be done, but it requires to determine numerous chemical data concerning the degradation of adequate solid compounds. Thus, experimental measurements of the degradation of nitrogenated compounds, such as HCN polymers or hexamethylenetetramine ($C_6H_{12}N_4$), have to be performed in order to test this hypothesis.

Acknowledgements

We are very grateful to Dominique Bockelée-Morvan for the helpful discussion. We thank Nicolas Biver for his permission to use unpublished results from his thesis. We also thank our two referees, D.G. Schleicher and D. Despois for their corrections and help in improving this manuscript.

References

A'Hearn, M.F., Millis, R., Festou, M., Benvenuti, P., Cacciari, C., Cassatella, A., Talavera, A., Wamsteker, W., Green, D.W.E., Hale, A., Marsden, B.G., 1983. Comet IRAS-Araki-Alcock (1983d). IAU Circ., 3802.

A'Hearn, M.F., Hoban, S., Birch, P.V., Bowers, C., Martin, R., Klinglesmith, D.A., 1986a. Cyanogen jets in comet Halley. Nature 324, 649–651.

A'Hearn, M.F., Hoban, S., Birch, P.V., Bowers, C., Martin, R., Klinglesmith, D.A., 1986b. Gaseous jets in comet P/Halley. In: 20th ESLAB Symposium, ESA SP 250, Heidelberg, pp. 483–486.

A'Hearn, M.F., Millis, R.L., Schleicher, D.G., Osip, D.J., Birch, P.V., 1995. The ensemble properties of comets: results from narrowband photometry of 85 comets, 1976–1992. Icarus 118, 223–270.

Arpigny, C., Jehin, E., Manfroid, J., Hutsemekers, D., Schultz, R., Stuwe, J.A., Zucconi, J.-M., Ilyin, I., 2003. Anomalous nitrogen isotope ratio in comets. Science 301, 1522–1524.

Biver, N., 1997. Molécules mères cométaires: observations et modélisations. Ph.D. Thesis, Université de Paris 7.

Biver, N., Bockelée-Morvan, D., Colom, P., Crovisier, J., Germain, B., Lellouch, E., Davies, J.K., Dent, W.R.F., Moreno, R., Paubert, G., Wink, J., Despois, D., Lis, D.C., Mehringer, D., Benford, D., Gardner, M., Phillips, T.G., Gunnarsson, M., Rickman, H., Winnberg, A., Bergman, P., Johansson, L.E.B., Rauer, H., 1999a. Long-term evolution of the outgassing of comet Hale-Bopp from radio observations. Earth Moon Planets 78, 5–11.

Biver, N., Bockelée-Morvan, D., Crovisier, J., Davies, J.K., Matthews, H.E., Wink, J.E., Rauer, H., Colom, P., Dent, W.R.F., Despois, D., Moreno, R., Paubert, G., Jewitt, D., Senay, M., 1999b. Spectroscopic monitoring of comet C/1996 B2 (Hyakutake) with the JCMT and IRAM radio telescopes. Astron. J. 118, 1850–1872.

Biver, N., Bockelée-Morvan, D., Colom, P., Crovisier, J., Henry, F., Lellouch, E., Winnberg, A., Johansson, L.E.B., Gunnarsson, M., Rickman, H., Rantakyrö, F., Davies, J.K., Dent, W.R.F., Paubert, G., Moreno, R., Wink, J., Despois, D., Benford, D.J., Gardner, M., Lis, D.C., Mehringer, D., Phillips, T.G., Rauer, H., 2002. The 1995–2002 long-term monitoring of comet C/1995 O1 (Hale-Bopp) at radio wavelength. Earth Moon Planets 90, 5–14.

Bockelée-Morvan, D., Crovisier, J., 1985. Possible parents for the cometary CN radical: photochemistry and excitation conditions. Astron. Astrophys. 151, 90–100.

Bockelée-Morvan, D., Crovisier, J., Baudry, A., Despois, D., Perault, M., Irvine, W.M., Schloerb, F.P., Swade, D., 1984. Hydrogen cyanide in comets—excitation conditions and radio observations of comet IRAS-Araki-Alcock 1983d. Astron. Astrophys. 141, 411–418.

Bockelée-Morvan, D., Crovisier, J., Despois, D., Forveille, T., Gerard, E., Schraml, J., Thum, C., 1987. Molecular observations of comets P/Giacobini-Zinner 1984e and P/Halley 1982i at millimetre wavelengths. Astron. Astrophys. 180, 253–262.

Bockelée-Morvan, D., Crovisier, J., Gérard, E., 1990. Retrieving the coma gas expansion velocity in P/Halley, Wilson (1987 VII) and several other comets from the 18-cm OH line shapes. Astron. Astrophys. 238, 382–400.

Bockelée-Morvan, D., Lis, D.C., Wink, J.E., Despois, D., Crovisier, J., Bachiller, R., Benford, D.J., Biver, N., Colom, P., Davies, J.K., Gerard, E., Germain, B., Houde, M., Moreno, R., Paubert, G., Phillips, T.G., Rauer, H., 1999. New molecules found in comet C/1995 O1 (Hale-Bopp). Investigating the link between cometary and interstellar material. Astron. Astrophys. 353, 1101–1114.

Boehnhardt, H., Drechsel, H., Vanysek, V., Waha, L., 1989. Photometric investigation of comets Bradfield 1987S and P/Borelly. Astron. Astrophys. 220, 286–292.

Bruston, P., Poncet, H., Raulin, F., Cossart-Magos, C., Courtin, R., 1989. UV spectroscopy of Titan's atmosphere, planetary organic chemistry, and prebiological synthesis I. Absorption spectra of gaseous propynenitrile and 2-butynenitrile in the 185- to 250-nm region. Icarus 78, 38–53.

Catalano, F.A., Baratta, G.A., Lo Presti, C., Strazzulla, G., 1986. Pre-perihelion photometry of P/Halley (1982i) at Catania (Italy) Observatory. Astron. Astrophys. 168, 341–345.

Churyumov, K.I., Rosenbush, V.K., 1991. Peculiarities of gas and dust production rates in Comets P/Halley (1986 III), P/Giacobini-Zinner (1985 XIII), P/Hartley-Good (1985 XVII) and P/Thiele (1985 XIX). Astron. Nachr. 312, 385–391.

Clairemidi, J., Moreels, G., Krasnopolsky, V.A., 1990a. Gaseous CN, C2, and C3 jets in the inner coma of Comet P/Halley observed from the VEGA 2 spacecraft. Icarus 86, 115–128.

Clairemidi, J., Moreels, G., Krasnopolsky, V.A., 1990b. Spectro-imagery of P/Halley's inner coma in the OH and NH ultraviolet bands. Astron. Astrophys. 231, 235–240.

Clarke, D.W., Ferris, J.P., 1995. Photodissociation of cyanoacetylene: application to the atmospheric chemistry of Titan. Icarus 115, 119–125.

Cochran, A.L., 1985. A re-evaluation of the Haser model scale lengths for comets. Astron. J. 90, 2609–2614.

Cochran, A.L., Schleicher, D.G., 1993. Observational constraints on the lifetime of cometary H_2O. Icarus 105, 235–253.

Combi, M.R., 1978. Convolution of cometary brightness profiles by circular diaphragms. Astron. J. 83, 1459–1466.

Combi, M.R., 1989. The outflow speed of the coma of Halley's comet. Icarus 81, 41–50.

Combi, M., 2002. Hale-Bopp: what makes a big comet different? Coma dynamics: observations and theory. Earth Moon Planets 89, 73–90.

Combi, M.R., Delsemme, A.H., 1980a. Neutral cometary atmospheres. I—an average random walk model for photodissociation in comets. Astrophys. J. 237, 633–640.

Combi, M.R., Delsemme, A.H., 1980b. Neutral cometary atmospheres. II—the production of CN in comets. Astrophys. J. 237, 641–645.

Combi, M.R., Delsemme, A.H., 1986. Neutral cometary atmospheres v. C_2 and CN in comets. Astrophys. J. 308, 472–484.

Combi, M.R., Fink, U., 1993. P/Halley—effects of time-dependent production rates on spatial emission profiles. Astrophys. J. 409, 151–162.

Combi, M., Huang, B., Cochran, A., Fink, U., Schulz, R., 1994. Time-dependent analysis of 8 days of CN spatial profiles in comet P/Halley. Astrophys. J. 435, 870–873.

Combi, M.R., Kabin, K., DeZeeuw, D.L., Gombosi, T.I., Powell, K.G., 1997. Dust–gas interrelations in comets: observations and theory. Earth Moon Planets 79, 275–306.

Cook, P.A., Langford, S.R., Ashfold, M.N.R., Dixon, R.N., 2000. Angular resolved studies of the Lyman-photodissociation of HCN and DCN: new dynamical insights. J. Chem. Phys. 113, 994–1004.

Cosmovici, C.B., Schwartz, G., Ip, W., Mack, P., 1988. Gas and dust jets in the inner coma of comet Halley. Nature 332, 705–709.

Cottin, H., Gazeau, M.C., Raulin, F., 1999. Cometary organic chemistry: a review from observations, numerical and experimental simulations. Planet. Space Sci. 47, 1141–1162.

Cottin, H., Benilan, Y., Gazeau, M.-C., Raulin, F., 2004. Origin of cometary extended sources from degradation of refractory organics on grain: polyoxymethylene as formaldehyde parent molecule. Icarus 167, 397–416.

Crovisier, J., 1987. Rotational and vibrational synthetic spectra of linear parent molecules in comets. Astron. Astrophys. Suppl. 68, 223–258.

Crovisier, J., 1994. Photodestruction rates for cometary parent molecules. J. Geophys. Res. 99, 3777–3781.

Crovisier, J., Despois, D., Bockelée-Morvan, D., Gerard, E., Paubert, G., Johansson, L.E.B., Ekelund, L., Winnberg, A., Ge, W., Irvine, W.M., Kinzel, W.M., Schloerb, F.P., 1990. A search for the millimetre lines of HCN in Comets Wilson 1987 VII and Machholz 1988 XV. Astron. Astrophys. 234, 535–538.

Crovisier, J., Bockelée-Morvan, D., Colom, P., Despois, D., Paubert, G., 1993. A search for parent molecules at millimetre wavelengths in comets Austin 1990V and Levy 1990 XX: upper limits for undetected species. Astron. Astrophys. 269, 527–540.

Delsemme, A.H., Combi, M.R., 1983. Neutral cometary atmospheres. IV—brightness profiles in the inner coma of comet Kohoutek 1973 XII. Astrophys. J. 271, 388–397.

Despois, D., Crovisier, J., Bockelée-Morvan, D., Gerard, E., Schraml, J., 1986. Observations of hydrogen cyanide in comet Halley. Astron. Astrophys. 160, L11–L12.

Eberhardt, P., Krankowsky, D., Schulte, W., Dolder, U., Lammerzahl, P., Berthelier, J.J., Woweries, J., Stubbeman, U., Hodges, R.R., Hoffman, J.H., Illiano, J.M., 1987. The CO and N_2 abundance in comet P/Halley. Astron. Astrophys. 187, 481–484.

Festou, M.C., Barale, O., Davidge, T., Stern, S.A., Tozzi, G.P., Womack, M., Zucconi, J.M., 1998. Tentative identification of the parent of CN radicals in comets: C_2N_2. BAAS 30, 1089.

Fink, U., Combi, M.R., 2004. The effect of using different scale lengths on the production rates of Comet 46P/Wirtanen. Planet. Space Sci. 52, 573–580.

Fink, U., Combi, M.R., Disanti, M.A., 1991. Comet P/Halley—spatial distributions and scale lengths for C_2, CN, NH_2, and H_2O. Astrophys. J. 383, 356–371.

Goidet-Devel, B., Clairemidi, J., Rousselot, P., Moreels, G., 1997. Dust spatial distribution and radial profile in Halley's inner coma. Icarus 126, 78–106.

Guo, J., Eng, R., Carrington, T., Filseth, S., 2000. Photodissociation of HCN at 157 nm: energy disposal in the CN ($A^2\Pi$) fragment. J. Chem. Phys. 112, 8904–8909.

Halpern, J.B., 1987. The photochemistry of some possible cometary CN parent species. ESA SP-278, 159–162.

Halpern, J.B., Yuhuia, H., 1997. Radiative lifetimes, fluorescence quantum yields and photodissociation of the C_2N_2 ($A^1\Sigma_u$) and ($B^1\Delta_u$) states: evidence for sterically hindered, triplet mediated crossings to the ($X^1\Sigma_g$) ground state. Chem. Phys. 222, 71–86.

Halpern, J.B., Miller, G.E., Okabe, H., 1988. The UV photochemistry of cyanoacetylene. J. Photochem. Photobiol. 42, 63–72.

Haser, L., 1957. Distribution d'intensité dans la tête d'une comète. Bull. Acad. R. Belg. 43, 740–750.

Huebner, W.F., Carpenter, C.W., 1979. Solar photo rate coefficients. Los Alamos Sci. Lab. LA-8085-MS, 94.

Huebner, W.F., Buhl, D., Snyder, L.E., 1974. HCN radio emission from Comet Kohoutek 1973f. Icarus 23, 580–584.

Huebner, W.F., Keady, J.J., Lyon, S.P., 1992. Solar photo rates for planetary atmospheres and atmospheric pollutants. Astrophys. Space Sci. 195, 1–289.

Jackson, W.M., 1976. Laboratory observations of the photochemistry of parent molecules: a review. In: Donn, B., Mumma, M., Jackson, W., A'Hearn, M.A., Harrington, R. (Eds.), The Study of Comets. NASA Spec. Publ. SP-393, pp. 679–704.

Jackson, W.M., 1991. Recent laboratory photochemical studies and their relationship to the photochemical formation of cometary radicals. In: Newburn, Jr., R.L., et al. (Eds.), Comets in the Post-Halley Era. Kluwer Academic Publishers, Dordrecht, pp. 313–332.

Jehin, E., Manfroid, J., Cochran, A.L., Arpigny, C., Zucconi, J.-M., Hutsemékers, D., Cochran, W.D., Endl, M., Schulz, R., 2004. The anomalous 14N/15N ratio in comets 122/P 1995 S1 (De Vico) and 153P/2002 C1 (Ikeya-Zhang). Astrophys. J. 613, L161–L164.

Jewitt, D.C., Matthews, H.E., Owen, T.C., Meier, R., 1997. Measurements of $^{12}C/^{13}C$, $^{14}N/^{15}N$ and $^{32}S/^{34}S$ in comet Hale-Bopp (C/1995 O1). Science 278, 90–93.

Kanda, K., Nagata, T., Ibuki, T., 1999. Photodissociation of some simple nitriles in the extreme vacuum ultraviolet region. Chem. Phys. 243, 89–96.

Kissel, J., Sagdeev, R.Z., Bertaux, J.L., Angarov, V.N., Audouze, J., Blamont, J.E., Buchler, K., Evlanov, E.N., Fechtig, H., Fomenkova, M.N., VonHoerner, H., Inogamov, N.A., Khromov, V.N., Knabe, W., Krueger, F.R., Langevin, Y., Leonas, V.B., Levasseur-Regourd, A.C., Managadze, G.G., Podkolzin, S.N., Shapiro, V.D., Tabaldyev, S.R., Zubkov, B.V., 1986. Composition of comet Halley dust particles from Vega observations. Nature 321, 280–282.

Klavetter, J.J., A'Hearn, M.F., 1994. An extended source for CN jets in comet P/Halley. Icarus 107, 322–334.

Krasnopolsky, V.A., 1991. C_3 and CN parents in comet P/Halley. Astron. Astrophys. 245, 310–315.

Krasnopolsky, V.A., Tkachuk, A.Y., Korablev, O.I., 1991. CN and C_3 distributions in comet P/Halley measured by the Vega 2 spectrometer TKS. Astron. Astrophys. 245, 662–668.

Lara, L.-M., Licandro, J., Oscoz, A., Motta, V., 2003. Behaviour of comet 21P/Giacobini-Zinner during the 1998 perihelion. Astron. Astrophys. 399, 763–772.

Larson, S.M., Hergenrother, C.W., Randt, J.C., 1997. The spatial and temporal distribution of CO^+ and CN in C/1995 O1 (Hale-Bopp). BAAS, 1036.

Lederer, S.M., Campins, H., 2001. Modeling coma gas jets in comet Hale-Bopp. In: 32nd Annual Lunar and Planetary Science Conference, March 12–16, 2001, Houston, TX, Abstract No. 1421.

Lederer, S.M., Campins, H., 2002. Evidence for chemical heterogeneity in the nucleus of C/1995 O1 Hale-Bopp. Earth Moon Planets 90, 381–389.

Lederer, S.M., Campins, H., Osip, D.J., Schleicher, D.G., 1999. Gaseous jets in comet Hale-Bopp (1995 O1). Earth Moon Planets 78, 131–136.

Magdziarz, P., Winiarski, M., Waniak, W., 1995. CN photometry of comet Levy 1900XX. Icarus 116, 40–45.

Magee-Sauer, K., Mumma, M.J., DiSanti, M.A., Dello Russo, N.D., Rettig, T.W., 1999. Infrared spectroscopy of the ν_3 band of hydrogen cyanide in comet C/1995 O1 Hale-Bopp. Icarus 142, 498–508.

Magee-Sauer, K., Mumma, M.J., DiSanti, M.A., Dello Russo, N.D., 2002. Hydrogen cyanide in comet C/1996/B2 Hyakutake. JGR (Planets) 107, E11 6-1.

Manfroid, J., Jehin, E., Hutsemékers, D., Cochran, A., Zucconi, J.-M., Arpigny, C., Schulz, R., Stüwe, J.A., 2005. Isotopic abundance of nitrogen and carbon in distant comets. Astron. Astrophys. 432, L5–L8.

Meredith, N.P., Wallis, M.K., Rees, D., 1992. Narrow-band IPD images of cometary CN and C_2—the effect of solar activity on coma scales. Mon. Not. R. Astron. Soc. 254, 693–704.

Millar, T.J., Rawlings, J.M.C., Bennet, A., Brown, P.D., Charnley, S.B., 1991. Gas phase reactions and rate coefficients for use in astrochemistry. The UMIST ratefile. Astron. Astrophys. Suppl. Ser. 87, 585–619.

Morley, G.P., Lambert, I.R., Ashfold, M.N.R., Rosser, K.N., Western, C.M., 1992. Dissociation dynamics of HCN(DCN) following photoexcitation at 121.6 nm. J. Chem. Phys. 97, 3157–3165.

Mueller, B.E.A., Samarasinha, N.H., Belton, M.J.S., 1999. Imaging the structure and evolution of the coma morphology of comet C/1995 O1 (Hale-Bopp). Earth Moon Planets 77, 181–188.

Newburn, R.L., Spinrad, H., 1984. Spectrophotometry of 17 comets. I—the emission features. Astron. J. 89, 289–309.

Newburn, R.L., Spinrad, H., 1989. Spectrophotometry of 25 comets—post-Halley updates for 17 comets plus new observations for eight additional comets. Astron. J. 97, 552–569.

O'Dell, C.R., Osterbrock, D.E., 1962. Emission-band and continuum photometry of comet Seki (1961f). Astrophys. J. 136, 559–566.

Petrie, S., Millar, T.J., Markwick, A.J., 2003. NCCN in TMC-1 and IRC+10216. Mon. Not. R. Astron. Soc. 341, 609–616.

Randall, C.E., Schleicher, D.G., Ballou, R.G., Osip, D.J., 1992. Observational constraints on molecular scalelengths and lifetimes in comets. BAAS 24, 1002.

Rauer, H., Helbert, J., Arpigny, C., Benkhoff, J., Bockelée-Morvan, D., Boehnhardt, H., Colas, F., Crovisier, J., Hainaut, O., Jorda, L., Kueppers, M., Manfroid, J., Thomas, N., 2003. Long-term optical

spectrophotometric monitoring of comet C/1995 O1 (Hale-Bopp). Astron. Astrophys. 397, 1109–1122.

Rodgers, S.D., Charnley, S.B., 1998. HNC and HCN in comets. Astrophys. J. 501, L227–L230.

Rodgers, S.D., Charnley, S.B., 2001. On the origin of HNC in comet Lee. Mon. Not. R. Astron. Soc. 323, 84–92.

Schleicher, D.G., Osip, D.J., 2002. Long- and short-term photometric behavior of comet Hyakutake (1996 B2). Icarus 159, 210–233.

Schleicher, D.G., Millis, R.L., Birch, P.V., 1987. Photometric observations of comet P/Giacobini-Zinner. Astron. Astrophys. 187, 531–538.

Schleicher, D.G., Millis, R.L., Thompson, D.T., Birch, P.V., Martin, R., Tholen, D.J., Piscitelli, J.R., Lark, N.L., Hammel, H.B., 1990. Periodic variations in the activity of comet P/Halley during the 1985/1986 apparition. Astron. J. 100, 896–912.

Schleicher, D.G., Millis, R.L., Osip, D.J., Birch, P.V., 1991. Comet Levy (1990c)—groundbased photometric results. Icarus 94, 511–523.

Schleicher, D.G., Lederer, S.M., Millis, R.L., Farnham, T.L., 1997. Photometric behavior of comet Hale-Bopp (C/1995 O1) before perihelion. Science 275, 1913–1915.

Schleicher, D.G., Millis, R.L., Birch, P.V., 1998. Narrowband photometry of comet P/Halley: variation with heliocentric distance, season, and solar phase angle. Icarus 132, 397–417.

Schloerb, F.P., Kinzel, W.M., Swade, D.A., Irvine, W.M., 1986. HCN production from comet Halley. Astrophys. J. 310, 55–60.

Schulz, R., A'Hearn, M.F., Birch, P.V., Bowers, C., Kempin, M., Martin, R., 1993. CCD imaging of Comet Wilson (1987VII)—a quantitative coma analysis. Icarus 104, 206–225.

Tatum, J.B., 1984. Cyanogen radiance/column-density ratio for comets calculated from the Swings effect. Astron. Astrophys. 135, 183–187.

Umbach, R., Jockers, K., Geyer, E.H., 1998. Spatial distribution of neutral and ionic constituents in comet P/Halley. Astron. Astrophys. Suppl. 127, 479–495.

Waniak, W., Magdziarz, P., Winiarski, M., 1994. Narrowband photometry of comet Austin 1990V. Icarus 108, 92–102.

Winnberg, A., Ekelund, E., Ekelund, A., 1987. Detection of HCN in comet 1P/Halley. Astron. Astrophys. 172, 335–341.

Womack, M., Lutz, B.L., Wagner, R.M., 1994. Pre- and post-perihelon abundances of gas and dust in comet Halley. Astrophys. J. 433, 886–894.

Woodney, L.M., A'Hearn, M.F., Schleicher, D.G., Farnham, T.L., McMullin, J.P., Wright, M.C.H., Veal, J.M., Snyder, L.E., Pater, I.D., Forster, J.R., Palmer, P., Kuan, Y.J., Williams, W.R., Cheung, C.C., Smith, B.R., 2002. Morphology of HCN and CN in comet Hale-Bopp (1995 O1). Icarus 157, 193–204.

Woods, T.N., Tobiska, W.K., Rottman, G.J., Worden, J.R., 2000. Improved solar lyman alpha irradiance modeling from 1947 through 1999 based on UARS observations. J. Geophys. Res. 105, 27195–27216.

Yung, Y.L., Allen, M., Pinto, J.P., 1984. Photochemistry of the atmosphere of Titan: comparison between model and observations. Astrophys. J. Suppl. Ser. 55, 465.